432–449 *Nucleic Acids Research, 2019, Vol. 47, No. 1* *Published online 5 November 2018*
doi: 10.1093/nar/gky1087

Dom34 mediates targeting of exogenous RNA in the antiviral OAS/RNase L pathway

Takuto Nogimori[1,†], Kyutatsu Nishiura[1,†], Sho Kawashima[1,†], Takahiro Nagai[1], Yuka Oishi[1], Nao Hosoda[1], Hiroaki Imataka[2], Yoshiaki Kitamura[3], Yukio Kitade[3] and Shin-ichi Hoshino[1,*]

[1]Department of Biological Chemistry, Graduate School of Pharmaceutical Sciences, Nagoya City University, Nagoya 467-8603, Japan, [2]Department of Materials Science and Chemistry and Molecular Nanotechnology Research Center, Graduate School of Engineering, University of Hyogo, Himeji 671-2201, Japan and [3]Department of Biomolecular Science, Graduate School of Engineering, Gifu University, 1-1 Yanagido, Gifu 501-1193, Japan

Received July 31, 2018; Revised October 11, 2018; Editorial Decision October 12, 2018; Accepted October 19, 2018

ABSTRACT

The 2′-5′-oligoadenylate synthetase (OAS)/RNase L pathway is an innate immune system that protects hosts against pathogenic viruses and bacteria through cleavage of exogenous single-stranded RNA; however, this system's selective targeting mechanism remains unclear. Here, we identified an mRNA quality control factor Dom34 as a novel restriction factor for a positive-sense single-stranded RNA virus. Downregulation of Dom34 and RNase L increases viral replication, as well as half-life of the viral RNA. Dom34 directly binds RNase L to form a surveillance complex to recognize and eliminate the exogenous RNA in a manner dependent on translation. Interestingly, the feature detected by the surveillance complex is not the specific sequence of the viral RNA but the 'exogenous nature' of the RNA. We propose the following model for the selective targeting of exogenous RNA; OAS3 activated by the exogenous RNA releases 2′-5′-oligoadenylates (2–5A), which in turn converts latent RNase L to an active dimer. This accelerates formation of the Dom34-RNase L surveillance complex, and its selective localization to the ribosome on the exogenous RNA, thereby promoting degradation of the RNA. Our findings reveal that the selective targeting of exogenous RNA in antiviral defense occurs via a mechanism similar to that in the degradation of aberrant transcripts in RNA quality control.

INTRODUCTION

In eukaryotes, mRNA turnover has three well-established roles of biological significance; (i) control of gene expression, (ii) mRNA quality control and (iii) antiviral defense. Cumulative evidence by recent transcriptome analyses has revealed that the mRNA turnover greatly contributes to the level of gene expression (1). In general, mRNA is degraded by the deadenylation-dependent 5′ to 3′ exonucleolytic decay pathway (2,3), in which deadenylation is the first and rate-limiting step in the decay of mRNA (4,5), and therefore, constitutes one of the most efficient steps for the control of gene expression. We have previously reported that mRNA decay is triggered by translation termination and proposed a model for the initiation of mRNA decay: after translation termination, the termination factors eRF1–eRF3 dissociate from PABP bound to the 3′ poly(A) tail, and in turn, Pan2–Pan3 and Caf1–Ccr4 deadenylases associate with PABP, which leads to the activation of the deadenylases and shortening of the poly(A) tail (6,7). Consistent with this model, recent studies demonstrated that mRNAs are degraded co-translationally (8,9).

In addition to the turnover of normal mRNA, mRNA decay plays key roles in mRNA quality control that recognizes and degrades aberrant mRNAs. The most well-studied quality control mechanism is nonsense-mediated mRNA decay (NMD). NMD is a surveillance mechanism that accelerates degradation of mRNAs with premature termination codons (PTCs) (for review see (10,11)). When the translating ribosome reaches the PTC, the termination factors eRF1–eRF3 in complex with Upf1 recognize the termination codon at the A site of the ribosome to trigger endo- and exo-nucleolytic degradation of the message (12). mRNA lacking in-frame termination codons is eliminated by nonstop mRNA decay (NSD) (13,14). As nonstop mRNA is translated, the ribosome enters the 3′ poly(A) tail of the mRNA and stalls at the 3′ end. In this case, other members of the translation termination factor family, Ski7 and/or Hbs1 in complex with Dom34, recognize the empty A site of the ribosome and recruit exosomes to degrade the mRNA (14–16). Furthermore, mRNA with the structural propensity to cause the ribosome to stall is eliminated by

*To whom correspondence should be addressed. Tel: +81 52 836 3427; Fax: +81 52 836 3427; Email: hoshino@phar.nagoya-cu.ac.jp
†The authors wish it to be known that, in their opinion, the first three authors should be regarded as Joint First Authors.

no-go decay (NGD). Hbs1–Dom34 enters the A site of the stalled ribosome and triggers endonucleolytic cleavage of the mRNA (17). The mechanism of NGD is characterized in yeast but not in mammals. It is noteworthy that irrespective of whether the mRNA is normal or aberrant, cellular mRNA is co-translationally degraded and members of the translation termination factor family play central roles in the initiation of mRNA decay.

On the other hand, mRNA decay plays pivotal roles in innate immunity by eliminating exogenous viral and bacterial mRNAs. In mammals, the canonical 2′-5′-oligoadenylate synthetase (OAS)/RNase L system has been established as a major antiviral defense mechanism (18). OAS/RNase L constitutes an innate immune system that responds to dsRNA, a pathogen-associated molecular pattern, to induce degradation of viral RNAs. In response to the dsRNA, OAS converts ATP to produce an unusual series of 2′-5′ oligoadenylates (2–5A), which act as a second messenger to trigger dimerization and activation of latent RNase L. RNase L endonuclease cleaves viral single-stranded RNA to limit viral replication (19,20). Although the OAS/RNase L system has been extensively investigated since its discovery in 1970s (21–25), an important question as to how the OAS/RNase L system selectively recognizes and discriminates exogenous RNA from cellular RNA to be eliminated (26–28) has yet to be elucidated.

Here, we show that a surveillance system involving Dom34 discriminates exogenous mRNA in a manner dependent on translation. Dom34 binds to form a complex with RNase L and recruits it to exogenous mRNAs, which leads to the rapid decay of the exogenous mRNAs. Our results provide an answer to the long-standing question as to how exogenous mRNA is discriminated from cellular mRNA and selectively targeted for degradation.

MATERIALS AND METHODS

Plasmids

To construct pUC18-EMCV-Rbz-R16D and pUC18-EMCV-(1–1B)-Rbz, the corresponding regions of pUC18-EMCV-Rbz (29) were amplified by inverse PCR using the primer pair KN030/KN032 and KN34/KN42, respectively, and pUC18-EMCV-Rbz as a template. pBK-5F-EGFP, a template for *in vitro* synthesis of mRNA, was constructed as follows. EGFP cDNA was PCR amplified using the primer pair NH733/NH732 and pCMV-5×Flag-EGFP (30) as a template, and inserted into XhoI and EcoRI sites of pBluscript II SK(–) (Agilent Technologies) to construct pBK-5×Flag-EGFP. β-globin 3′-UTR that contains 72 nts poly(A) tail was then PCR amplified using the primer pair NH734/NH770 and pFlag-CMV/TO-BGG (6) as a template, and inserted into EcoRI and BamHI sites of pBK-5×Flag-EGFP. pBK-EGFP (1–87) control and ATG mt, templates for *in vitro* synthesis of mRNA, were constructed as follows. Firstly, pBK-5F-EGFP-2 was constructed by inverse PCR using the primer pair TN0024/TN0025 and pBK-5F-EGFP as a template. Secondly, to construct pBK-EGFP (1–30), the corresponding region of EGFP (1–30) cDNA was PCR amplified using the primer pair TN0022/TN0023 and pEGFPc1 (Clontech) as a template, and inserted into XhoI and XbaI sites of pBK-5F-EGFP-2. Thirdly, pEGFPc1 (D37 silent mt) was constructed by inverse PCR using the primer pair TN0029/TN0030 and pEGFPc1 as a template. Finally, the corresponding region of EGFP (1–87) cDNA and EGFP (1–87) ATG mt cDNA were PCR amplified using the primer pair TN0026/TN0031 and TN0022/TN0031, respectively, and pEGFPc1 (D37 silent mt) as a template, and inserted into XhoI and EcoRI sites of pBK-EGFP (1–30) pA. To construct pUC18-Rbz-IRES, the corresponding region of IRES cDNA was amplified by inverse PCR using the primer pair TN0088/TN0089 and pUC18-Rbz-EMCV as a template. To construct pUC18-IRES-5F-EGFP-EMCV-UTR, EGFP cDNA was PCR amplified using the primer pair M13+/TN0091 and pBK-5F-EGFP as a template, and inserted into XhoI and NotI sites of pUC18-Rbz-IRES. To construct pUC18-IRES-5F-EGFP-BGG-UTR, EGFP cDNA was PCR amplified using the primer pair M13+/M13– and pBK-5F-EGFP as a template, and inserted into XhoI and NotI sites of pUC18-Rbz-IRES. pCMV-TO-5×Flag-EGFP was constructed as follows. pCMV-TO-β-globin 3′-UTR was amplified by inverse PCR using the primer pair TN0094/TN0095 and pFlag-CMV/TO-BGG as a template. 5×Flag-EGFP cDNA was then PCR amplified using the primer pair TN0092/TN0093 and pBK-5F-EGFP as a template, and inserted into XbaI and SalI sites of pCMV-TO-β-globin 3′-UTR. To construct pCMV-5×Flag-Dom34 and pCMV-5×Myc-Dom34, cDNA encoding Dom34 was PCR amplified using the primer pair NH0275/NH0276 and pFlag-Dom34 (16) as a template, and inserted into EcoRI site of pCMV-5×Flag (31) and pCMV-5×Myc (30), respectively. To construct pCMV-5×Flag-RNase L, cDNA encoding RNase L was amplified by RT-PCR using the primer pair YH033/YH034 and HeLa total RNA as a template, and inserted into EcoRI and EcoRV sites of pCMV-5×Flag. To construct pCMV-5×Myc-RNase L, pCMV-5×Flag-RNase L was digested by EcoRI and XhoI, and the resulting fragment was inserted into EcoRI and XhoI sites of pCMV-5 ×Myc. To construct pCMV-5 × Flag-eRF1, cDNA encoding eRF1 was PCR amplified using the primer pair NH0592/NH0593 and pFlag-eRF1 (32), and inserted into EcoRI and XhoI sites of pCMV-5×Flag. To construct pCMV-5×Flag-RNase L Y312A, the corresponding region of RNase L cDNA was amplified by inverse PCR using the primer pair TN0047/TN0048 and pCMV-5×Flag-RNase L as a template. To construct pCMV-5×Myc-PABPC1, cDNA encoding PABPC1 was PCR amplified using the primer pair NH0347/NH0348 and pGEX6P1-PABP (33) as a template. The resulting fragment was digested with BamHI and SalI, and inserted into pCMV-5×Myc. To construct pCMV-5×Myc-OAS3, cDNA encoding OAS3 was amplified by RT-PCR using the primer pair TN0060/TN0061 and HeLa total RNA as a template, and inserted into HindIII and EcoRV sites of pCMV-5×Myc. To construct pCold-OAS3 (743–1087 a.a.), the corresponding region of OAS3 (743–1087 a.a.) cDNA was amplified by PCR using the primer pair TN0081/TN0062 and pCMV-5×Myc-OAS3 as a template, and inserted into HindIII and XbaI sites of pCold-I (TAKARA). pCold-S2-PF was constructed by inverse PCR using the primer pair NH0804/NH0805 and pCold-ProS2

(TAKARA) as a template. pCold-S2-PM was constructed by inverse PCR using the primer pair NH0876/NH0877 and pCold-ProS2 (TAKARA) as a template. To construct pCold-S2-Flag-RNase L, pCMV-5×Flag-RNase L was digested by EcoRI and XhoI, and the resulting fragment was inserted into EcoRI and SalI sites of pCold-S2-PF. To construct pCold-S2-Myc-Dom34, cDNA encoding Dom34 was PCR amplified using the primer pair NH0275/NH0276 and pFlag-Dom34 (16) as a template, and inserted into EcoRI site of pCold-S2-PM. The 5×Flag epitope tagging donor against endogenous RNase L gene (p5×Flag-RNase L-Donor) was constructed as follows. Firstly, to construct pP2A, a self-cleaving P2A sequence was generated by hybridization of oligonucleotides TN0184/TN0185, and the resulting fragment was inserted into EcoRI and EcoRV sites of pBluscript II SK(–). Secondly, to construct pP2A-5F, 5×Flag epitope tag was PCR amplified using the primer pair TN0166/CMV6 and pCMV-5×Flag as a template, and the resulting fragment was inserted into EcoRV and HindIII sites of pP2A. Thirdly, to construct pPuro-P2A-5F, Puromycine resistance gene was PCR amplified using the primer pair TN0189/TN0192 and AAVS1_Puro_PGK1_3×FLAG_Twin_Strep (Addgene plasmid # 68375) as a template, and the resulting fragment was inserted into EcoRI and BamHI sites of pPuro-P2A-5F. Fourthly, to construct p5arm-Puro-P2A-5F, the 5′ homology arm was PCR amplified using the primer pair TN0205/TN0206 and HeLa genome as a template, and the resulting fragment was inserted into XbaI and BamHI sites of pPuro-P2A-5F. Finally, to construct p5×Flag-RNase L-Donor, the 3′ homology arm was PCR amplified using the primer pair TN0207/TN0208 and HeLa genome as a template, and the resulting fragment was inserted into XhoI and KpnI sites of p5arm-Puro-P2A-5F. To construct pgRNA-RNase L expressing sgRNA, inverse PCR was performed using gRNA_AAVS1-T2 (Addgene plasmid # 41818) and the primer pair TN0231/TN0232. hCas9 was a gift from Dr George Church (Addgene plasmid # 41815), AAVS1_Puro_PGK1_3×FLAG_Twin_Strep was a gift from Dr Yannick Doyon and gRNA_AAVS1-T2 was a gift from Dr George Church through Addgene. Primer sequences are listed in Table 1.

siRNA

siRNA sequences are listed in Table 2.

In vitro mRNA synthesis

EMCV–RNA, EMCV-R16D-RNA, EMCV-1B-RNA, IRES-5×Flag-EGFP-EMCV-UTR mRNA and IRES-5×Flag-EGFP-BGG-UTR mRNA were synthesized using the RiboMAX kit (Promega) according to the manufacturer's instructions. pUC18-EMCV-Rbz (29), pUC18-EMCV-Rbz-R16D, pUC18-EMCV-(1–1B)-Rbz and pUC18-IRES-5F-EGFP-EMCV-UTR that were linearized by SalI were used as templates for the *in vitro* synthesis of EMCV–RNA, EMCV-R16D-RNA, EMCV-1B-RNA and IRES-5×Flag-EGFP-EMCV-UTR mRNA, respectively. pUC18-IRES-5×F-EGFP-BGG- UTR that was linearized by BsmBI was used as a template for the *in vitro* synthesis of IRES-5×F-EGFP-BGG-UTR mRNA. 5×Flag-EGFP mRNA, EGFP (1–87) mRNA control and EGFP (1–87) mRNA AUG mt were synthesized using T7 RNA polymerase (TAKARA) according to the manufacturer's instructions. pBK-5F-EGFP, pBK-EGFP (1–87) control and pBK-EGFP (1–87) ATG mt that were linearized by BsmBI were used as templates for the *in vitro* synthesis of 5×Flag-EGFP, EGFP (1–87) mRNA control and EGFP (1–87) mRNA AUG mt, respectively. For the synthesis of mRNA whose 5′-terminus was modified with a cap structure, 3′-O-Me-m7G(5′)ppp(5′)G cap analog (New England Biolabs) was added during the T7 polymerase reaction. Following DNase I treatment, the synthetic RNAs were purified using a illustra MicroSpin G-25 column (GE Healthcare) or illustra MicroSpin S-400 HR column (GE Healthcare) and quantified using NanoDrop One (Thermo Fisher Scientific). The synthetic RNAs were further purified using denaturing gel to confirm that the RNA preparation contains no detectable dsRNA byproduct from the T7 polymerase reactions and results obtained using the synthetic RNAs were not due to the dsRNA contaminants (Supplementary Figure S7).

Cell culture and transfection

HeLa cells and T-REx HeLa cells were cultured in Dulbecco's modified Eagle's medium (Nissui) supplemented with 5% fetal bovine serum. Transfection of siRNA and *in vitro* transcribed RNA was performed using Lipofectamine 2000 (Invitrogen), Lipofectamine RNAi MAX (Invitrogen) or Lipofectamine MessengerMAX (Invitrogen) according to the manufacturer's instructions. Transfection of plasmid DNA was performed using Polyethyleneimine MAX (Polysciences) according to the manufacturer's instructions. Transfection of 2–5A was performed using Neon™ Transfection System (Invitrogen).

Preparation of a virus stock and viral titer determination

To prepare an EMCV stock, BHK-21 cells were infected with EMCV particles (strain Rueckert, GenBank accession no. M81861) (29). After three days, the infected cells were harvested and lysed, and viruses were prepared by three freeze-thaw cycles to release EMCV virions. The titer of EMCV was measured using plaque assay (29). Confluent BHK-21 cells on a 60-mm dish were incubated with the diluted viral sample (1 ml) for 1 h. Following removal of the medium, an agar-containing medium (0.5 ml agar (2.5% in water, Difco) plus 2 ml medium) was overlaid on the cells. After agar layer became solid (∼30 min at room temperature), 2.5 ml of medium was overlaid, and incubated for 30 h at 37°C. Plaques formed on each dish were counted, and plaque-forming units (pfu) were calculated.

Northern blot analysis

For analyzing replication of EMCV, HeLa cells were transfected with siRNA for 24 h. The cells were further treated with IFN-α/β for 24 h and infected with EMCV at MOI = 1. The cells were harvested at the specified time after the infection. For analyzing decay of *in vitro*

Table 1. Primers used in this study

Name	Sequence
CMV6	5′-ATTCTAGTTGTGGTTTGTCC-3′ (antisense)
GEX-R	5′-TTCCCAGTCACGACGTTGTAA-3′ (antisense)
KN22	5′-ACAGACCTTGCATTCCTTTGGCGA-3′ (antisense)
KN23	5′-AGAGGAACTGCTTCCTTCACGACA-3′ (antisense)
KN24	5′-CAGACGTTGTTTGTCTTCAAGAAGC-3′ (antisense)
KN25	5′-TTGTTGAATACGCTTGAGGAGAGC-3′ (antisense)
KN30	5′-GATAAAACAGCACTACGCCCCACCGTT-3′ (sense)
KN32	5′-TGGTACGTGAATACGGGGCCCATC-3′ (antisense)
KN34	5′-TAGTAGTGTAGTCACTGGCACAAC -3′ (sense)
KN42	5′-CTGTCTAGAAAGTGTCTCATG-3′ (antisense)
M13+	5′-GTAAAACGACGGCCAGTGAGC-3′ (sense)
M13-	5′-AACAGCTATGACCATGATTAC-3′ (antisense)
NH0208	5′-CTTATCGTCGTCATCCTTGTAATC-3′ (sense)
NH0273	5′-TTCGAATTCATGGCCCGGCATCGGAATGTT-3′ (sense)
NH0275	5′-TCCGAATTCATGAAGCTCGTGAGGAAGAAC-3′ (sense)
NH0276	5′-GGCGAATTCTTAATCCTCTTCAGAACTGGA-3′ (antisense)
NH0347	5′-TAGCGGATCCATGAACCCCAGTGCCCCCAG-3′ (sense)
NH0348	5′-CCCTGAGTCGACTTAAACAGTTGGAACACC-3′ (antisense)
NH0406	5′-ACAGTAGAGCTCTCCCCTATACTAGGTTAT-3′ (sense)
NH0592	5′-GGCGAATTCATGGCGGACGACCCCAGTGC-3′ (sense)
NH0593	5′-GTCCTCGAGCTAGTAGTCATCAAGGTCA-3′ (antisense)
NH0732	5′-ATCGAATTCAAGCTTAGTACAGCTCGTCCATGCC-3′ (antisense)
NH0733	5′ -ACCCTCGAGCCCACCATGGCATCAATGGAT-3′ (sense)
NH0734	5′-CTTGAATTCGATATCGTCGACGCTCGCTTTCTTGCTGTCCAATTTCT-3′ (sense)
NH0770	5′-GTCTCT(72)CTAGACATCATTGCAATGAAAA-3′ (antisense)
NH0804	5′-GATGACGACGATAAGGGATCCGAATTCAAGCTTGTC-3′ (sense)
NH0805	5′-CTTGTAATCCAGGGGCCCCTGGAACAGAACTTCCAG-3′ (antisense)
NH0849	5′-GCCGTTTACGTCGCCGTCCAGCTC -3′ (antisense)
NH0850	5′-GATGAACTTCAGGGTCAGCTTGCC -3′ (antisense)
NH0876	5′-TCAGAGGAGGACCTGGGATCCGAATTCAAGCTTGTC -3′ (sense)
NH0877	5′-GATCAGCTTCTGCAGGGGCCCCTGGAACAGAACTTCCAG -3′ (antisense)
NH0956	5′-GGTGAAGGTCGGAGTCAACG -3′ (sense)
NH0957	5′-TGGGTGGAATCATATTGGAA -3′ (antisense)
TN0016	5′-CTCATTGTAGAAGGTGTGGTGCCA-3′ (antisense)
TN0017	5′-AGGCGTACAGGGATAGCACAGCCT-3′ (antisense)
TN0018	5′-GAGGATCTTCATGAGGTAGTCAGT-3′ (antisense)
TN0019	5′-TTGCGGATGTCCACGTCACACTTC-3′ (antisense)
TN0022	5′-GACCTCGAGATCGTGAGCAAGGGCGAGGAG-3′ (sense)
TN0023	5′-GCCTCTAGAGATATCGAATTCAAGCTTACACGCTGAACTTGTGGCCGTT-3′ (antisense)
TN0024	5′-ACCGCGGTGGAGCTCCAGCTT-3′ (sense)
TN0025	5′-GCTCTTGAACTAGTGGATCGT-3′ (antisense)
TN0026	5′-GACCTCGAGATGGTGAGCAAGGGCGAGGAG-3′ (sense)
TN0027	5′-GAACAGCTCCTCGCCCTTGCTCAC -3′ (antisense)
TN0029	5′-GCCACCTACGGCAAGCTGACC-3′ (sense)
TN0030	5′-GCCACCTACGGCAAGCTGACC-3′ (sense)
TN0031	5′-TTCGAATTCTTAGGACTTGAAGAAGTCGTGCTGCTTCCCGTGGT-3′ (antisense)
TN0047	5′-GCCGACCATTCCCTTGTGAAGGTT-3′ (sense)
TN0048	5′-ATTCCGCCTCGCTGTCATAACAAG-3′ (antisense)
TN0060	5′-CGGAAGCTTATGGACTTGTACAGCACCCCG-3′ (sense)
TN0061	5′-ATCTCACACAGCAGCCTTCACTGG-3′ (antisense)
TN0062	5′-TTCTCTAGATCACACAGCAGCCTTCACTGG-3′ (antisense)
TN0081	5′-TGGAAGCTTATGCCAGCCCTCCTTTACCAA-3′ (sense)
TN0088	5′-CTCCTCGAGCATGGTTGTGGCCAT-3′ (antisense)
TN0089	5′-TAGGCGGCCGCTAGTGTAGTCACTGGCAC -3′ (sense)
TN0091	5′-CGAGCGGCCGCTTAGTACAGCTCGTCCATG-3′ (antisense)
TN0092	5′-CACTCTAGAGCGAATTGGGTACCGGGCCCC-3′ (sense)
TN0093	5′-AGCGAGCGTCGACGATATCGA-3′ (antisense)
TN0094	5′-TCTGACGGTTCACTAAACTCTAGAGATCTC-3′ (antisense)
TN0095	5′-TAAGTCGACTTTCTTGCTGTCCAATTTCTA-3′ (sense)
TN0166	5′-ACCGATATCGCCACCATGGCATCAATGGAT-3′ (sense)
TN0172	5′-GCGCCCCACCAAGCTCAAGA-3′ (sense)
TN0173	5′-GCTCCCTCGCTCCCAAGCAT-3′ (antisense)
TN0174	5′-ACCCGAACAGTTCCCCCTGGT-3′ (sense)
TN0175	5′-ACAAGGGTACCATCGGAGTTGCC -3′ (antisense)
TN0176	5′-TGCTGCCAGCCTTTGACGCC -3′ (sense)
TN0177	5′-TTCGCCCGCATTGCTGTAGCTG-3′ (antisense)
TN0184	5′-AATTCGGAAGCGGAGCTACTAACTTCAGCCTGCTGAAGCAGGCTGGAGACGTGGAGGAGAA CCCTGGACCTGAT-3′ (sense)
TN0185	5′-ATCAGGTCCAGGGTTCTCCTCCACGTCTCCAGCCTGCTTCAGCAGGCTGAAGTTAGTAGCTC CGCTTCCG -3′ (antisense)
TN0189	5′-TCTGAATTCGGCACCGGGCTTGCGGGTCAT-3′ (antisense)
TN0192	5′-GGCGGATTCACCGAGTACAAGCCCACGGTG -3′ (sense)

Table 1. Continued

Name	Sequence
TN0205	5′-CGGCCGCTCTAGAACTAGTGGCACAGGGTTGTACAAAGAGGACA-3′ (sense)
TN0206	5′-GCTTGTACTCGGTGGATCCCATGACGGTAAATGCCACCTGCTAC-3′ (antisense)
TN0207	5′-CGATACCGTCGACCTCGAGGAGAGCAGGGATCATAACAACCCCC-3′ (sense)
TN0208	5′-ATTGGGTACCGGGCCCCCCCTTCAGCAGGAGGGTGAAAATCTTC-3′ (antisense)
TN0231	5′-GACGGTAAATCGGTGTTTCGTCCTTTCCAC-3′ (antisense)
TN0232	5′-ATGGAGAGCAGTTTTAGAGCTAGAAATAGC-3′ (sense)
TN0235	5′-TAAATTAGAGACAATTTGAAC-3′ (sense)
TN0238	5′-TGTGCCACGCTTGCTAATGAT-3′3′ (antisense)
TN0241	5′-GCCGAAAACCCGGTATCCCGGGTTCTTAAAACAGCCTGTGGGTT-3′ (sense)
TN0242	5′-CTTTCGGCCTCATCAGTTAAAACACCCTATAGTGAGTCGTATTA-3′ (antisense)
TN0243	5′-AACAACCTGTCAATTGTCACC-3′ (antisense)
TN0244	5′-AATTTACCTGGGTCTTGAGTG -3′ (antisense)
TN0280	5′-GGTTGTGGTAATGTTTGAGCG-3′ (antisense)
YH033	5′-CTTGAATTCATGGAGAGCAGGGATCATAACAAC-3′ (sense)
YH034	5′-ATCTCAGCACCCAGGGCTGGCCAACCC-3′ (antisense)

Table 2. siRNAs used in this study

Name	Sequence
Luciferase	5′-r(CGU ACG CGG AAU ACU UCG A)d(TT)-3′
Dom34 #1	5′-r(CAU CCA AGA GAA UGA GUA U)d(TT)-3′
Dom34 #2	5′-r(GCA GUG GGA UAG UGU GGU A)d(TT)-3′
Dom34 #3	5′-r(GCA GUG AAG ACC GAC AAC A)d(TT)-3′
RNase L	5′-r(GCU GUU CAA AAC GAA GAU G)d(TT)-3′
OAS3	5′-r(GAA GGA UGC UUU CAG CCU A)d(TT)-3′
Ski2	5′-r(GGA GAU AGA CUU UGA GAA A)d(TT)-3′
Mtr4	5′-r(GAG UCA AUA ACU GAA GAC U)d(TT)-3′
Caf1	5′-r(CAU CUG GUA UCC AGU UUA A)d(TT)-3′
Pan2	5′-r(GUC AAU GGC AGU GAU GAU A)d(TT)-3′
Lsm1	5′-r(GGA CCG AGG UCU UUC CAU U)d(TT)-3′
Dcp2	5′-r(CAU AUG GUG CAA UUA UUC U)d(TT)-3′
Upf1	5′-r(GAU GCA GUU CCG CUC CAU U)d(TT)-3′
ABCE1	5′-r(GAU UCU AGA AGA UGA CCU A)d(TT)-3′
OAS1	5′-r(CUA CAG AGA GAC UUC CUG A)d(TT)-3′
OAS2	5′-r(CGC UCU GAG CUU AAA UGA U)d(TT)-3′

synthesized mRNA, HeLa cells were transfected with siRNA for 48 h to downregulate the specified proteins. The cells were transfected with EMCV-R16D-RNA, EMCV-1B-RNA, IRES-5×Flag-EGFP-EMCV-UTR mRNA. IRES-5×Flag-EGFP-BGG-UTR mRNA, 5×Flag-EGFP mRNA or EGFP (1–87) mRNA for 3 h, washed with phosphate-buffered saline to completely remove the *in vitro* synthesized mRNA, and harvested at the specified time after the transfection. For the transcriptional shut off analysis, T-REx HeLa cells were transfected with siRNA against either luciferase (control), Dom34 or RNase L. At 24 h, after siRNA transfection, the cells were further transfected with pCMV-TO-5×Flag-EGFP. At 6 h after plasmid transfection, EGFP mRNA expression was induced by treatment with tetracycline (10 ng/ml) for 18 h, and the cells were harvested at the specified time after the transcription was shut off. Total RNA was isolated and analyzed by northern blotting using either [^{32}P] or [^{33}P]-labeled Flag nucleotide (NH0208), EMCV-5′ UTR nucleotides (KN22/KN23/KN24/KN25), EGFP nucleotides (NH0849/NH0850/TN0027) or β-actin nucleotides (TN0016/TN0017/TN0018/TN0019) as probes. The levels of mRNAs were quantitated from the northern blot using Image Gauge Ver 4.23 (Fujifilm) or ImageJ 10.2. Entire gels stained with ethidium bromide are shown in Supplementary Figure S5.

Endogenous gene tagging in HeLa cells

HeLa/5×Flag-RNase L cells were obtained as follows. HeLa cells were transfected with hCas9 (Addgene plasmid # 41815), pgRNA-RNase L and p5×Flag-RNase L-Donor. Two days after transfection, cells were selected with 0.5 μg/ml puromycin and maintained as a polyclonal pool.

Immunoprecipitation and western blotting

For immunoprecipitation, cells were transfected with plasmids for 24 h. The cells were lysed in buffer A (20 mM Tris–HCl (pH 7.5), 50 mM NaCl, 2.5 mM EDTA, 0.5% Nonidet P-40, 1 mM DTT, 0.1 mM PMSF, 2 μg/ml aprotinin, 2 μg/ml leupeptin and 2 μg/ml PepstatinA), buffer B (20 mM Tris–HCl (pH 7.5), 50 mM NaCl, 1 mM $MgCl_2$, 0.5% Nonidet P-40, 1 mM DTT and 5 mg/ml cOmplete mini (Roche)) or buffer C (20 mM Tris–HCl (pH 7.5), 50 mM NaCl, 0.5% Nonidet P-40, 1 mM DTT, 5 mg/ml cOmplete mini (Roche) and 40 U/ml Recombinant RNase inhibitor (TAKARA)) on ice for 10 or 30 min. The cell extract was centrifuged at 20,400 × g for 10 min, and the supernatant was subsequently incubated with anti-Flag M2 agarose (Sigma, A2220) or anti-c-Myc agarose affinity gel antibody produced in rabbit (Sigma, A7470) in the presence of 1 μg/ml RNase A (Sigma) as needed at 10°C for

1 h. The agarose resin was then washed three times with each buffer. The retained proteins and RNAs were eluted using SDS-PAGE sample buffer and phenol/chloroform extraction, respectively. For immunoprecipitation assay of endogenous proteins, HeLa or HeLa/5×Flag-RNase L cells were lysed in buffer D (20 mM Tris–HCl (pH 7.5), 100 mM NaCl, 1 mM EDTA, 0.5% Nonidet P-40, 1 mM DTT, 10% glycerol, 0.25% sodium deoxycholate, 5 μg/ml RNase A and 1×protease inhibitor ocktail (nacalai tesque)) on ice for 30 min. The lysates were centrifuged at 20,400 × g for 20 min, and the supernatant was subsequently incubated with anti-Flag M2 agarose (Sigma) at 10°C for 1 h. The agarose resin was then washed three times with buffer D. The retained proteins were eluted using SDS-PAGE sample buffer and analyzed by western blotting. For analyzing total cell lysate by western blotting, proteins from total cell lysate were extracted with SDS-PAGE sample buffer. Antibodies used for western blotting were as follows: anti-Flag (Sigma, F3165, Cell Signaling Technology, 2368), anti-Myc (Roche, 11667149001, Santa Cruz Biotechnology, sc-789), anti-Dom34 ((16), raised against His-tagged Dom34(220–385)), anti-RNase L (raised against His-tagged RNase L(1–333)), anti-OAS3 (abcam, ab154270), anti-GAPDH (16), anti-Xrn1 (Bethyl Laboratories, A300–443A), anti-Ski2 (Proteintech, 11462–1-AP), anti-Mtr4 (Bethyl Laboratories, A300–614A) and anti-Upf1 (raised against a synthetic peptide corresponding to N-terminal residues of Upf1 (EEDEEDTYYTKDLPIHAC)). The levels of proteins in the siRNA treated conditions were determined by western blotting in Supplementary Figure S4.

Protein purification

6×His-OAS3 (743–1087 a.a.), 6×His-S2-Flag, 6×His-S2-Flag-RNase L and 6×His-S2-Myc-Dom34 were produced in *Escherichia coli* BL21 by adding bacterial expression vectors and 0.5 mM IPTG. The cells were lysed in buffer E (20 mM Na-Pi (pH 8.0), 300 mM NaCl, 1 mM DTT, 10 mM Imidazole) and the recombinant proteins were purified from the lysate. The lysates were affinity-purified using Ni-NTA agarose (QIAGEN).

Polysome profile analysis

Polysome profile analysis by sucrose density gradients was performed as follows. HeLa cells or HeLa/5×Flag-RNase L cells were harvested with 100 μg/ml cycloheximide/phosphate-buffered saline at the specified time after the mRNA or 2–5A transfection. The cells were lysed in buffer F (20 mM HEPES–KOH (pH 7.5), 1 mM EGTA, 5 mM $MgCl_2$, 150 mM KCl, 100 μg/ml cycloheximide, 0.5 mM PMSF, 0.5% Nonidet P-40, 2 μg/ml aprotinin, 2 μg/ml leupeptin, 2 μg/ml pepstatinA and 1 mg/ml heparin) or buffer G (20 mM HEPES–KOH (pH 7.5), 1 mM EGTA, 5 mM $MgCl_2$, 150 mM KCl, 100 μg/ml cycloheximide, 0.25% sodium deoxycholate, 1×protease inhibitor cocktail (nacalai tesque) and 1 mg/ml heparin) on ice for 10 min. The cell extract was centrifuged at 20,400 × g for 10 min, and the supernatant was layered onto linear 10–50% sucrose density gradients (20 mM HEPES–KOH (pH 7.5), 1 mM EGTA, 5 mM $MgCl_2$, 150 mM KCl, 100 μg/ml cycloheximide) and centrifuged at 24,000 rpm for 90 min using a Beckman JS-24 rotor or 39,000 rpm for 90 min using a Beckman SW41Ti rotor. After centrifugation, 500 μl fractions were collected using BIOCOMP Piston Gradient Fractionator.

OAS3 enzyme activity assay

A colorimetric method was performed to measure the amount of pyrophosphate (PP_i) with the production of 2–5A by OAS3 (34). Recombinant 6×His-OAS3 (743–1087 a.a.) protein and RNA were incubated for 1 h in the presence of 20 mM HEPES–NaOH (pH 7.5), 5 mM $MnCl_2$, 1 mM ATP and 4 mM DTT in a total volume of 20 μl at 37°C in a 384 plate. The reaction mixture was mixed with 20 μl of molybdate reagent (2.5% hexaammonium heptamolybdate tetrahydrate (Wako) in 2.5 M H_2SO_4) and 30 μl of Eikonogen Reagent (0.0357% of 1-amino-2-naphthol-4-sulfonic acid (Wako), 0.0357% of sodium sulfite (Wako), 2.09% of sodium bisulfite and 357 mM 2-mercaptoethanol (Wako)). This mixture was quantified by A_{580} mesurement with Wallac 1420 ARVO MX multilabel counter (PerkinElmer).

Statistical analysis

P-values were determined using the two-tailed Student's *t* test for paired samples. $^{*}P < 0.05$, $^{**}P < 0.01$. Error bars represent mean ± SEM.

RESULTS

Dom34 restricts EMCV replication

First, we searched for cellular host factors involved in defense against viral replication using a positive-sense single-stranded RNA virus, EMCV (encephalomyocarditis virus), as a model system. In particular, we focused on the mRNA decay factors, which are involved in the decay of cellular mRNA. HeLa cells were treated with previously validated siRNAs targeting each of the mRNA decay factors, and knockdown was allowed to proceed for 24 h, after which cells were treated with or without 25 U/ml of interferon (IFN)-α/β for 24 h. The cells were infected with EMCV at a multiplicity of infection (MOI) of 1, and the relative level of EMCV RNA was measured by northern blotting. Among the factors investigated, down-regulation of Dom34, RNase L or Upf1 significantly increased the level of EMCV RNA (Figure 1A). The effects were more prominent by the treatment with IFN-α/β. As RNase L and Upf1 are already known to be restriction factors for positive-strand RNA viruses (35,36), we focused on the newly identified Dom34 for further study.

Thus, we examined the effect of Dom34 depletion on the kinetics of EMCV replication. HeLa cells were depleted of either Dom34 or RNase L (positive control), after which cells were treated with or without 25 U/ml of IFN-α/β, and the cells were harvested over time after the viral infection. EMCV replication rate was increased by the down-regulation of Dom34 and RNase L as indexed by the level of EMCV RNA (Figure 1B). The effects were more prominent by the treatment with IFN-α/β. To rule out the possibility that Dom34 inhibited virus attachment and entry into cells,

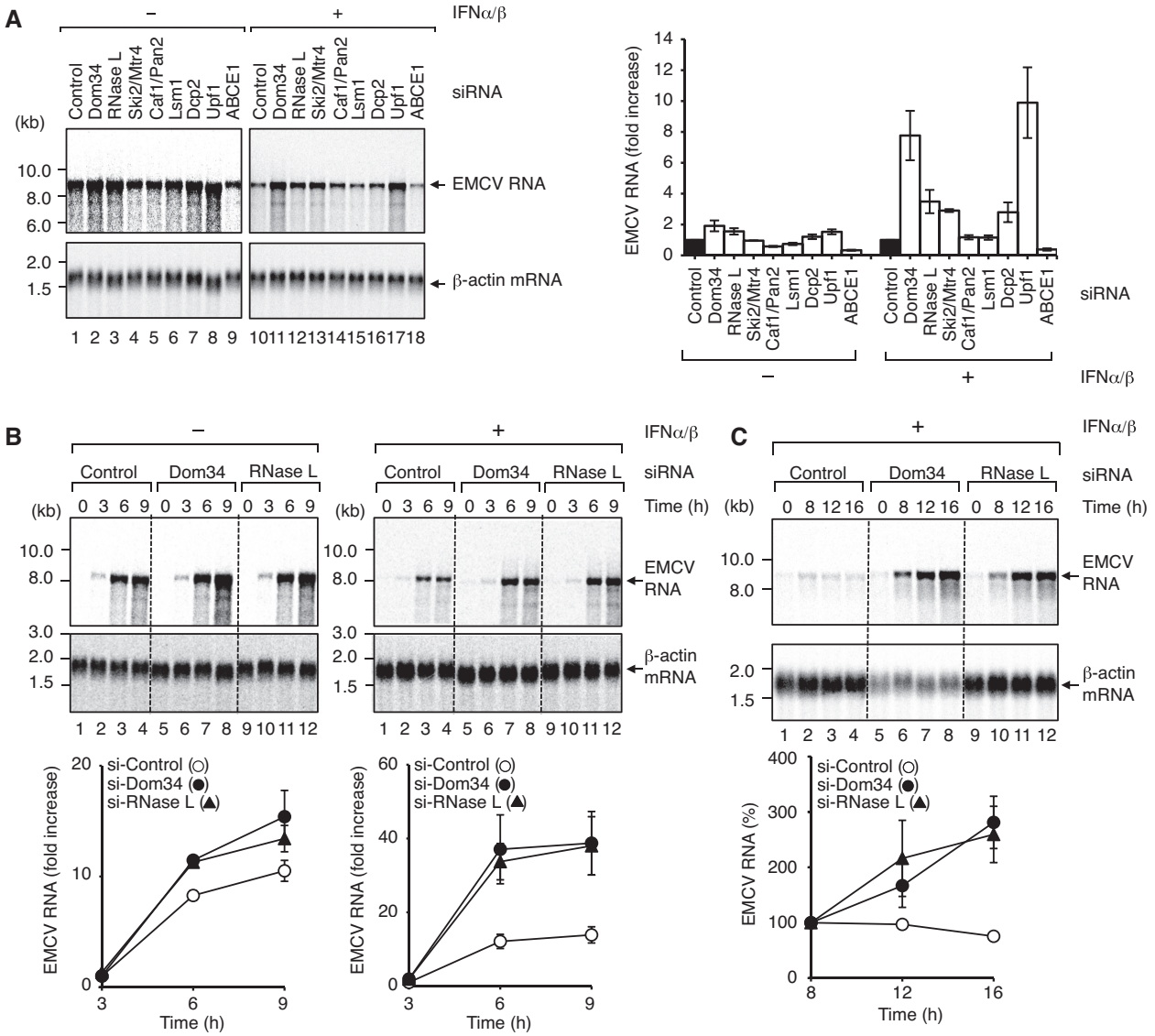

Figure 1. Identification of Dom34 as a novel restriction factor for EMCV replication. (**A**) HeLa cells were transfected with siRNA against either luciferase (control) or targets. At 24 h after siRNA transfection, the cells were treated with (lanes 10–18) or without (lanes 1–9) IFN-α/β (25 U/ml) for 24 h. The cells were infected with EMCV (MOI = 1 for 1 h). The cells were cultured in growth medium for 8 h, and RNA was analyzed by northern blotting. The levels of EMCV–RNA were quantified and normalized to the levels of β-actin mRNA, and the normalized levels of each control (lanes 1 and 10) were defined as 1 (mean ± SEM, $n = 4$). (**B**) HeLa cells were transfected with siRNA against either luciferase (control), Dom34 or RNase L. At 24 h after siRNA transfection, the cells were treated with (right panels) or without (left panels) IFN-α/β (25 U/ml) for 24 h and the cells were infected with EMCV (MOI = 1 for 1 h). The cells were cultured in growth medium over time. EMCV–RNA and β-actin mRNA were analyzed by northern blotting. The levels of EMCV–RNA were quantified and normalized to the levels of β-actin mRNA, and the normalized levels of the 3-hr time point of the control were defined as 1 (mean ± SEM, $n = 3$). (**C**) HeLa cells were transfected with siRNA against either luciferase (control), Dom34 or RNase L. At 24 h after transfection, the cells were treated with IFN-α/β (5 U/ml) for 24 h. The cells were further transfected with EMCV–RNA for 1 h. The cells were cultured in growth medium and harvested at the indicated times. RNA was analyzed by northern blotting. The levels of EMCV–RNA were quantified and normalized to the levels of β-actin mRNA, where the normalized levels from the 8-h time point were defined as 100% (mean ± SEM, $n = 3$).

we next analyzed EMCV replication by utilizing an *in vitro* EMCV replication system (37,38). EMCV RNA was synthesized by *in vitro* transcription and subsequently transfected into HeLa cells. In this condition, EMCV replication was suppressed by the host defense mechanism during a 16-h incubation (Figure 1C). However, robust increase in the level of EMCV RNA was observed by the down-regulation of Dom34 and RNase L. These results indicate that Dom34 as well as RNase L suppresses EMCV replication.

Downregulation of RNase L and Dom34 increases the half-life of EMCV RNA

Dom34 is known as a quality control factor eliminating aberrant mRNAs and plays a key role in triggering the non-stop and no-go mRNA decay (15–17,39,40). These results prompted us to investigate if Dom34 is involved in the decay of EMCV RNA. Therefore, we developed a method that measures the half-life of the EMCV RNA by constructing EMCV (EMCV-R16D) with a point mutation in the viral

RNA polymerase gene 3D (Figure 2A). As EMCV-R16D is unable to replicate its own viral RNA in cells, we can assess the half-life of EMCV RNA. In this condition, EMCV-R16D-RNA was decayed with a short half-life of 1.4 ± 0.2 h and RNase L depletion increased the half-life of EMCV-R16D-RNA (3.0 ± 0.4 h), which is consistent with previous results demonstrating that RNase L is an innate immune endoribonuclease against EMCV (Figure 2B, left panel). Similar results were obtained upon depletion of Dom34 (Figure 2B, right panel). These results suggest that Dom34 as well as RNase L is involved in the decay of EMCV RNA.

To further confirm that Dom34 functions in the decay of other viral RNAs, we measured the half-life of CVB1 (coxsackievirus B1) RNA by constructing CVB1 lacking nonstructural protein coding regions required for the viral replication (CVB1-VP1). HeLa cells were treated with siRNA against either Dom34 or RNase L for 48 h, after which cells were transfected with the CVB1-VP1-RNA, and RNA isolated from the cells was analyzed by northern blotting (Supplementary Figure S1A and S1B). Depletion of either Dom34 or RNase L increased the half-life of the CVB1-VP1-RNA. In contrast to EMCV and CVB1, we could not detect Dom34/RNase L dependency in the decay of poliovirus RNA, which is consistent with a previous report showing that poliovirus RNA has a phylogenetically conserved structure that is inhibitory to RNase L (data not shown) (41).

Dom34 detects the 'exogenous' nature of EMCV RNA

Previous studies reported that Dom34 detects the stalled ribosome on mRNAs with specific elements, such as secondary structure and rare codons, in the quality control system for eliminating aberrant mRNAs (17). This led us to speculate that EMCV RNA may have a structural element that induces ribosomal stall in the open reading frame of the viral RNA. To assess the region required for the Dom34-mediated decay of EMCV RNA, we constructed a series of deletion and replacement mutants of EMCV RNA (Figure 2A). As EGFP and β-globin genes are well-characterized and frequently used as reporters, we used EGFP-ORF and β-globin-3′ UTR for the gene replacement. HeLa cells were treated with siRNAs against either luciferase or Dom34 for 48 h, and then transfected with each of the EMCV mutants. The total RNA isolated from the cells was subjected to northern blotting. Contrary to what we expected, partial deletion of the EMCV ORF and even the complete replacement of the ORF to the EGFP ORF did not compromise the Dom34 dependency of the viral RNA decay. Dom34 knockdown increased the half-life of each RNA (Figure 2C, D). Therefore, we next searched the 3′-untranslated region (3′UTR) of EMCV RNA for the presence of elements required for the Dom34-mediated decay. We replaced the 3′UTR of EMCV RNA with that of the β-globin gene. As shown in Figure 2E, decay of the resultant IRES-5×Flag-EGFP-BGG-UTR was still dependent on Dom34. Finally, we replaced IRES-containing 5′-untranslated region (5′UTR) of EMCV with the 5′-capped-5′UTR of non-viral synthetic mRNA (5×Flag-EGFP). Surprisingly, even the replacement of the 5′UTR did not compromise the Dom34 dependency of the viral RNA decay (Figure 2F). From these results, we conclude that Dom34-mediated decay of EMCV RNA is not dependent on the sequence of the viral RNA, but may require the 'exogenous' nature of the RNA. It is noteworthy that RNase L also mediates the decay of the RNA construct. RNase L knockdown increased the half-life of the 5×Flag-EGFP RNA (see Figure 3).

It is reasonable to assume that both Dom34 and RNase L mediate decay of exogenous RNA irrespective of whether the RNA is derived from a virus or not. Indeed, the final replacement construct 5×Flag-EGFP mRNA used in the above experiment was 5' capped and 3′ polyadenylated mRNA, but contained no virus-derived RNA. To determine whether Dom34 discriminates 'exogenous/foreign' RNA, we constructed a EGFP expression plasmid, which endogenously produces 5′ capped and 3′ poly(A) tailed 5×Flag-EGFP mRNA, and compared the decay profile to that of the corresponding exogenous synthetic mRNA with the same sequence. T-REx HeLa cells were transfected with the plasmid and the decay kinetics of 5×Flag-EGFP mRNA derived from the plasmid were monitored using a tetracycline regulatory transcriptional chase approach. After transcription was induced by tetracycline for 18 h, the decay kinetics of the 5×Flag-EGFP mRNA were analyzed by northern blotting. Decay of the endogenously expressed 5×Flag-EGFP mRNA was not affected by the downregulation of Dom34 (Figure 2G). This is in sharp contrast to the exogenously introduced 5×Flag-EGFP mRNA (Figure 2F). Similar results were also observed for RNase L; exogenously introduced 5×Flag-EGFP mRNA but not endogenously expressed 5×Flag-EGFP mRNA was stabilized by RNase L downregulation (compare Figures 2H and 3E). These results clearly demonstrate that Dom34 as well as RNase L functions in the decay of exogenous mRNA.

Dom34 interacts with RNase L endoribonuclease

The above results demonstrate that Dom34 and RNase L are involved in the decay of exogenous mRNA. Thus, we expected that RNase L may form a complex with Dom34 to function in the decay of exogenous mRNA. Therefore, we first examined the interaction between Dom34 and RNase L. HeLa cells were transfected with a plasmid expressing 5×Flag-RNase L and a plasmid expressing either 5×Myc-Dom34 or 5×Myc-eRF1. Cell extracts were prepared and subjected to immunoprecipitation with an anti-Flag antibody. Western blot analysis showed that 5×Flag-RNase L co-purified with 5×Myc-Dom34, but not with 5×Myc-eRF1 (Figure 3A). Essentially the same results were obtained with or without RNase A treatment, indicating that the interaction is not mediated by RNA. To further explore the interaction between endogenous Dom34 and RNase L, we used CRISPR/Cas9-mediated Flag epitope tagging at the N-terminus of RNase L and performed immunoprecipitation with an anti-Flag antibody. As shown in Figure 3B, endogenous Flag-tagged RNase L co-purified with endogenous Dom34. To examine if the interaction was direct or not, we next constructed *E. coli* recombinant proteins, 6×His-S2-Myc-Dom34 and 6×His-S2-Flag-RNase L, and performed a pull-down experiment. 6×His-S2-Myc-Dom34 co-purified with 6×His-S2-Flag-RNase L (Figure

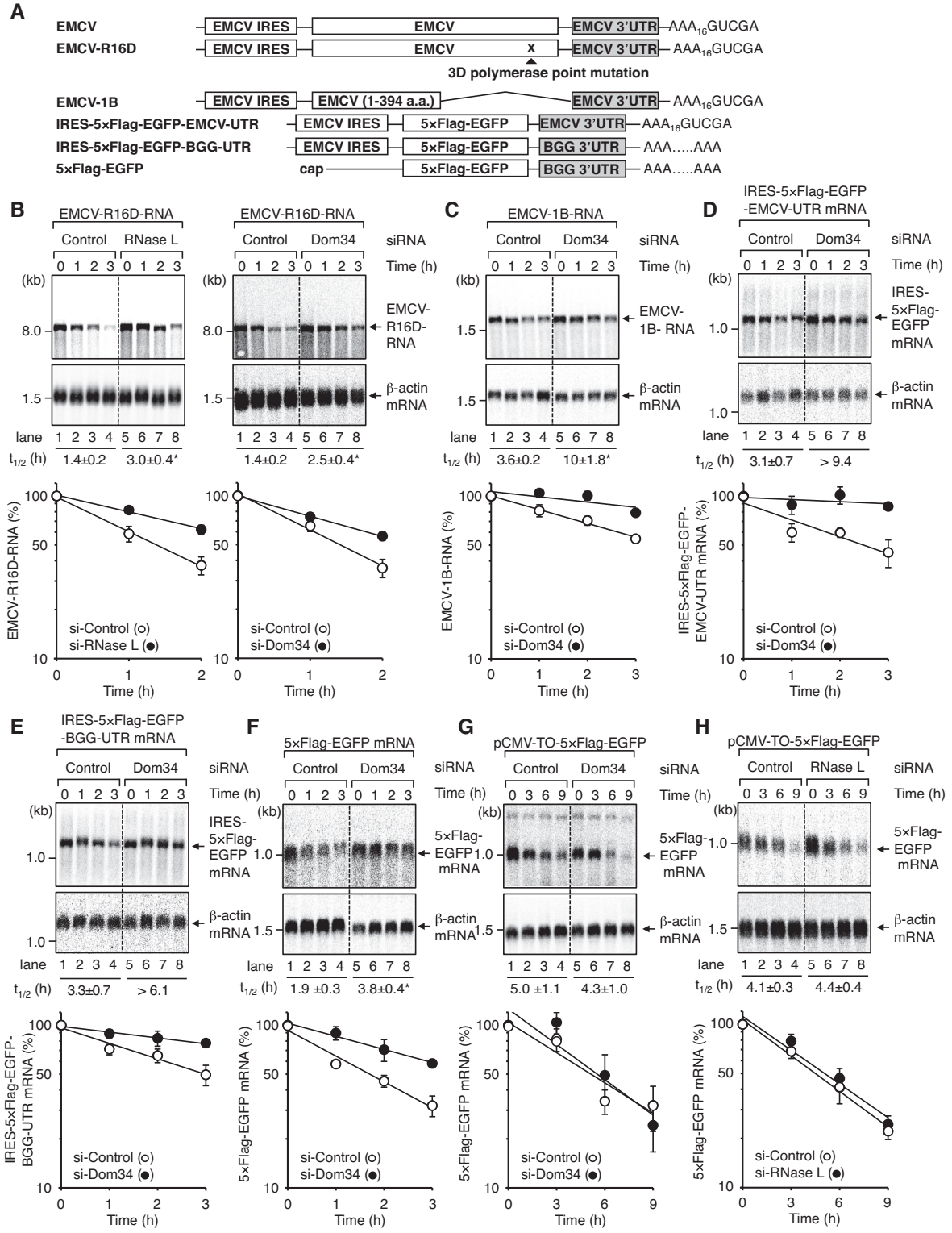

Figure 2. Dom34 and RNase L degrade EMCV RNA. (**A**) Schematic diagram of EMCV–RNA and its mutants. (**B**–**F**) Degradation rate of point mutant, deletion and replacement mutants of EMCV RNA in HeLa cells transfected with siRNA against either luciferase (control), Dom34 or RNase L. The levels of the RNAs that were normalized to the levels of β-actin mRNA were quantified, where the normalized levels from the 0-hr time point were defined as 100% (mean ± SEM). The half-lives of the RNAs were calculated (average $t_{1/2}$ ± SEM, $n = 3$ or 4). (**G**, **H**) T-REx HeLa cells were transfected with siRNA against either luciferase (control), Dom34 or RNase L. At 24 h after siRNA transfection, the cells were further transfected with pCMV-TO-5×Flag-EGFP. At 6 h after plasmid transfection, EGFP mRNA expression was induced by treatment with tetracycline (10 ng/ml) for 18 h, and the cells were harvested at the specified time after the transcription was shut off. The levels of 5×Flag-EGFP mRNA that were normalized to the levels of β-actin mRNA were quantified, where the normalized levels from the 0-hr time point were defined as 100% (mean ± SEM). The half-lives of the RNAs were calculated (average $t_{1/2}$ ± SEM, $n = 3$).

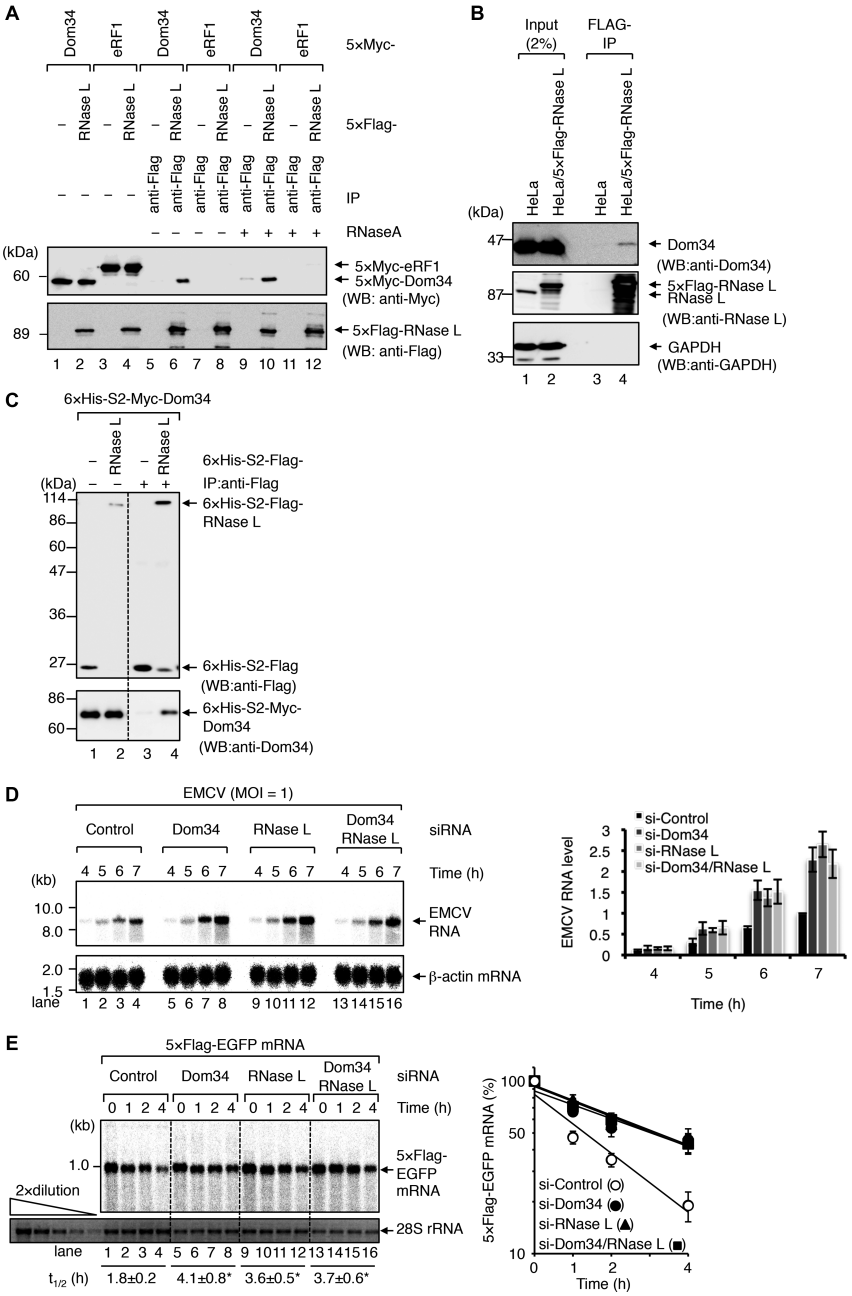

Figure 3. RNase L interacts with Dom34 and acts together to eliminate exogenous mRNA. (**A**) HeLa cells were transfected with a combination of either pCMV-5×Myc-Dom34 (lanes 1, 2, 5, 6, 9 and 10) or pCMV-5×Myc-eRF1 (lanes 3, 4, 7, 8, 11 and 12) and either pCMV-5×Flag (1, 3, 5, 7, 8 and 11) or pCMV-5×Flag-RNase L (2, 4, 5, 6, 10 and 12). The cells were lysed in lysis buffer A for 30 min on ice. The lysates were clarified by centrifugation for 10 min at 20,400 × g, and the supernatants were rotated with anti-Flag M2 agarose in the presence of 1 μg/ml RNase A as needed at 10°C for 1 h. The immunoprecipitates (lanes 5–12) and inputs (lanes 1–4, 10% of the amount immunoprecipitated) were analyzed by western blotting with the indicated antibodies. (**B**) Cell extracts prepared from HeLa cells and HeLa cells expressing Flag-tagged RNase L were used for co-immunoprecipitation. The immunoprecipitates (lanes 3 and 4) and inputs (lanes 1 and 2, 2% of the amount immunoprecipitated) were analyzed by western blotting with the indicated antibodies. (**C**) Either recombinant 6×His-S2-Flag (lanes 1 and 3) or 6×His-S2-Flag-RNase L (lanes 2 and 4) was incubated with 6×His-S2-Myc-Dom34 in buffer A at 10°C for 1 h. The immunoprecipitates (lanes 3 and 4) and inputs (lanes 1 and 2, 10% of the amount immunoprecipitated) were analyzed by western blotting with the indicated antibodies. (**D**) HeLa cells were transfected with siRNA against either luciferase (control), Dom34, RNase L or Dom34/RNase L. At 24 h after siRNA transfection, the cells were treated with IFN-α/β (25 U/ml) for 24 h and the cells were infected with EMCV (MOI = 1 for 1 h). The cells were cultured in growth medium over time. EMCV–RNA and β-actin mRNA were analyzed by northern blotting. The levels of EMCV–RNA were quantified and normalized to the levels of β-actin mRNA, and the normalized levels of the 7-h time point of the control were defined as 1 (mean ± SEM, $n = 3$). (**E**) HeLa cells were transfected with siRNA against either luciferase (control), Dom34, RNase L or Dom34/RNase L. At 48 h after siRNA transfection, the cells were further transfected with 5×Flag-EGFP mRNA for 3 h, and cultured in growth medium over time. 5×Flag-EGFP mRNA and 28S rRNA were analyzed by northern blotting (upper panel) and ethidium bromide staining (lower panel), respectively. The leftmost five lanes, which analyzed 2-fold dilutions of total RNA, show that the conditions used for ethidium bromide staining are semi-quantitative. The levels of 5×Flag-EGFP mRNA that were normalized to the levels of 28S rRNA were quantified, where the normalized levels from the 0-h time point were defined as 100% (mean ± SEM, $n = 4$). The half-lives of 5×Flag-EGFP mRNA were calculated (average $t_{1/2}$ ± SEM, $n = 4$).

3C). These results indicate that Dom34 directly binds to form a complex with RNase L.

Dom34 and RNase L act together to eliminate exogenous mRNA

The finding that Dom34 and RNase L directly bind to form a complex prompted us to investigate if these factors act together to eliminate exogenous mRNA using the double knockdown strategy. HeLa cells were depleted of Dom34 and/or RNase L for 24 h, after which cells were treated with 25 U/ml of interferon (IFN)-α/β for 24 h. The cells were infected with EMCV at a MOI of 1, and the relative level of EMCV RNA was measured by northern blotting (Figure 3D). Dom34 knockdown increased EMCV replication to a level comparable to that seen in RNase L knockdown. Of note, the increased EMCV replication by the single knockdown of either protein was not affected by the double knockdown of both proteins. Next, we assessed the decay rate of exogenous mRNA under the double knockdown condition. HeLa cells were depleted of Dom34 and/or RNase L for 48 h, after which cells were transfected with 5×Flag-EGFP mRNA, and RNA isolated from the cells was analyzed by northern blotting (Figure 3E). The RNase L knockdown increased the half-life of the exogenous mRNA to a level comparable to that seen in Dom34 knockdown. The increased half-life of the mRNA by the single knockdown of either protein was again not affected by the double knockdown of both proteins (Figure 3E). These results suggest that RNase L and Dom34 act together to eliminate exogenous mRNA.

Dom34-RNase L regulates exogenous mRNA decay downstream of OAS3

The above results demonstrate that the decay of exogenous mRNA involves Dom34-RNase L. To determine if catalytic activity of RNase L is required for the exogenous mRNA decay, we have examined the effect of a previously reported RNase L inhibitor, curcumin, on rapid degradation of transfected 5×Flag-EGFP mRNA. We first confirmed that curcumin inhibited RNase L activity with an IC_{50} of ∼30 μM in an *in vitro* enzyme assay using FRET (Supplementary Figure S2A) (42). At the near IC_{50} concentration, curcumin inhibited the exogenous mRNA decay: the half-life of the 5×Flag-EGFP mRNA was increased 3-fold from 1.4 h to 4.2 h (Supplementary Figure S2B). These results indicate that catalytic activity of RNase L is required for the exogenous mRNA decay. RNase L is an endoribonuclease that is activated through the 2′-5′-oligoadenylate synthetase (OAS) pathway to function in antiviral and antibacterial innate immunity. In the presence of dsRNA or ssRNA with secondary structures, OAS can be activated to catalyze the oligomerization of ATP into 2′,5′-linked oligoadenylate (2–5A), which in turn binds to and activates RNase L (18). Human cells express four related OAS family members: OAS1, OAS2, OAS3 and OASL (43). Among the OAS family members, OAS3 is an enzyme that senses long RNAs (44). This led us to speculate that the Dom34-mediated exogenous mRNA decay involves activation of OAS3. Thus, we investigated if OAS3 is involved in the decay of exogenous mRNA. HeLa cells were depleted of OAS3 and/or Dom34 for 48 h and then transfected with 5×Flag-EGFP mRNA. RNA isolated from the cells was analyzed by northern blotting (Figure 4A). Consistent with our expectation, OAS3 depletion stabilized exogenous mRNA to a level comparable to that seen in Dom34 depletion (Figure 4A). Moreover, the increased half-life by the single knockdown of either protein was not affected by the double knockdown of both proteins. The steady-state level of the exogenous 5×Flag-EGFP mRNA was 3-fold higher in OAS3-depleted cells than that in the control case (Figure 4B). We confirmed that OAS3 was specifically depleted by OAS3 siRNA (Supplementary Figure S3).

The aforementioned results indicate that Dom34-RNase L specifically mediates decay of exogenous mRNA, but not that of endogenously expressed mRNA. However, the interesting question that remains is how exogenous mRNA is recognized as 'exogenous'. We hypothesized that OAS3 is one candidate that discriminates exogenous mRNA to be degraded by Dom34-RNase L. To test this idea, we performed an RNA immunoprecipitation assay. HeLa cells were transfected with a plasmid expressing either 5×Myc-OAS3 or 5×Myc-PABPC1 (positive control) and either 5×Flag-EGFP mRNA or a plasmid expressing 5×Flag-EGFP mRNA. Northern blot analysis of anti-Myc immunoprecipitates showed that 5×Myc-PABP co-purified with 5×Flag-EGFP mRNA irrespective of whether it is exogenous or endogenous, whereas 5×Myc-OAS3 co-purified with exogenous 5×Flag-EGFP mRNA, but not with endogenously expressed 5×Flag-EGFP mRNA derived from the plasmid (Figure 4C). Thus, we expected that the binding of exogenous 5×Flag-EGFP mRNA to the OAS3 should activate 2′-5′ oligoadenylate synthetase activity. To test this prediction, we purified recombinant OAS3 to near homogeneity and measured the activity of OAS3 in the presence of 5×Flag-EGFP mRNA. The 5×Flag-EGFP mRNA activates 2′-5′ oligoadenylate synthetase activity to a level comparable to that seen with a well-known activator poly(I:C) (Figure 4D). These results suggest that OAS3 is responsible for the recognition of exogenous mRNA and transduction of signaling 2–5A molecule to the downstream RNase L. These results further substantiate our conclusion that Dom34-RNase L regulates the decay of exogenous mRNA downstream of OAS3.

Dom34 mediates exogenous mRNA decay in a manner dependent on translation

The above results demonstrate that OAS3 contributes to recognize exogenous mRNA and releases signaling 2–5A molecule to activate RNase L. However, it is still unclear how exogenous mRNA is targeted for degradation by the activated RNase L. In the mRNA quality control system eliminating aberrant mRNA, Dom34 plays a central role in targeting aberrant mRNA for degradation by NSD/NGD. Thus, we set out to elucidate the role of Dom34 in the decay of exogenous mRNA. In NSD/NGD, Dom34 mediates degradation of aberrant mRNA in a manner dependent on translation. To examine if degradation of exogenous mRNA also requires translation, we analyzed the effects of a translation inhibitor, cycloheximide (CHX), on the half-

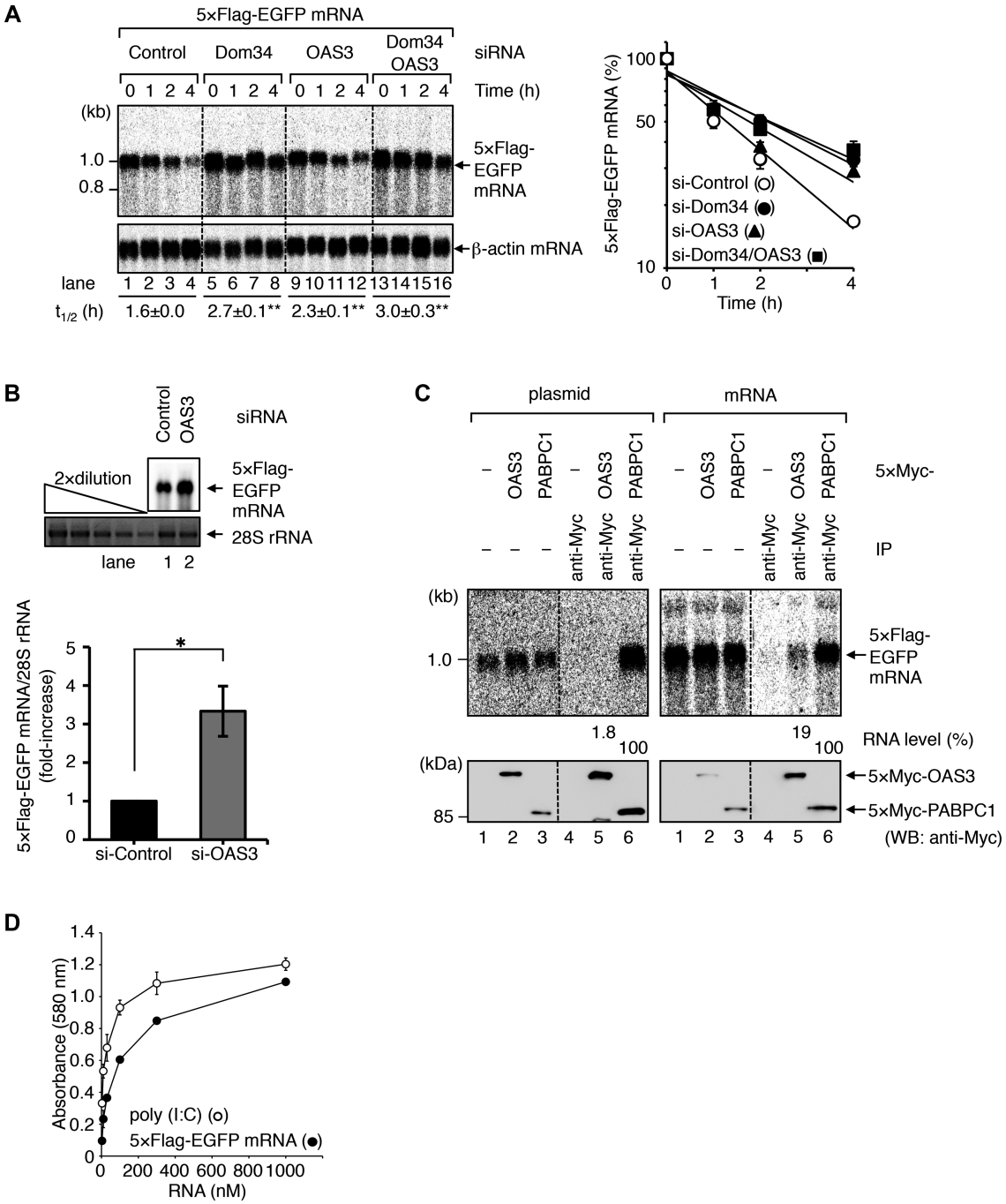

Figure 4. OAS3 functions in the decay of exogenous mRNA in mammalian cells. (**A**) HeLa cells were transfected with siRNA against either luciferase (control), Dom34, OAS3 or Dom34/OAS3. At 48 h after siRNA transfection, the cells were further transfected with 5×Flag-EGFP mRNA for 3 h, and cultured in growth medium over time. 5×Flag-EGFP mRNA and β-actin mRNA were analyzed by northern blotting. The levels of 5×Flag-EGFP mRNA that were normalized to the levels of β-actin mRNA were quantified, where the normalized levels from the 0-h time point were defined as 100% (mean ± SEM, $n = 4$). The half-lives of 5×Flag-EGFP mRNA were calculated (average $t_{1/2}$ ± SEM, $n = 4$). (**B**) The steady-state levels of 5×Flag-EGFP mRNA. HeLa cells were transfected with siRNA against either control luciferase (lane 1) or OAS3 (lane 2). At 48 h after siRNA transfection, the cells were further transfected with 5×Flag-EGFP mRNA. At 6 h after mRNA transfection, the cells were washed with phosphate-buffered saline to completely remove the 5 × Flag-EGFP mRNA and harvested at 7 h after the wash. Total cell lysate was analyzed by northern blotting (upper panel) and ethidium bromide staining (lower panel), respectively. The left most five lanes, which analyzed 2-fold dilutions of total RNA, show that the conditions used for ethidium bromide staining are semi-quantitative. The amount of 5×Flag-EGFP mRNA was measured and normalized to the 28S rRNA. The mRNA level in luciferase siRNA-treated cells was set to 1 and fold-increases are indicated. (**C**) HeLa cells were transfected with a combination of pCMV-TO-5×Flag-EGFP (left panels) or 5×Flag-EGFP mRNA (right panels) and either pCMV-5×Myc (lanes 1 and 4), pCMV-5×Myc-OAS3 (lanes 2 and 5) or pCMV-5×Myc-PABPC1 (lanes 3 and 6). The cells were lysed in buffer C. The immunoprecipitates (lanes 4–6) and inputs (lanes 1–3, 10% of the amount immunoprecipitated) were analyzed by northern blotting (upper panels) or western blotting (lower panels) with the indicated antibody. Values below the blots represent quantification of RNA levels. (**D**) Activation of recombinant OAS3 (743–1087 a.a.) by poly(I:C) or 5×Flag-EGFP mRNA. Purified OAS3 (743–1087 a.a.) (400 nM) and RNA were incubated in the presence of ATP (1 mM) and $MnCl_2$ (5 mM) at 37°C for 1 h. OAS3 activity was quantified by a molybdenum blue method. Error bars represent SEM for three independent experiments.

life of exogenous mRNA. HeLa cells were transfected with 5×Flag-EGFP mRNA for 3 h. The cells were treated with or without CHX over time and total RNA prepared from the cells was subjected to northern blot analysis. Cycloheximide treatment significantly increased the half-life of the exogenous mRNA from 1.8 ± 0.2 h to 3.3 ± 0.4 h (Figure 5A). To further confirm that the decay of exogenous mRNA was translation-dependent, we constructed an synthetic mRNA lacking the AUG initiation codon (EGFP(1–87) (AUG mt) mRNA) and analyzed the rate of mRNA decay. The exogenous mRNA lacking the initiation codon showed an increased half-life of 7.1 ± 0.8 h as compared with the control case with the initiation codon (3.9 ± 0.5 h) (Figure 5B). In this case, downregulation of Dom34 did not significantly affect the rate of the mRNA decay. These results further substantiate our conclusion that Dom34 mediates degradation of exogenous mRNA in a manner dependent on translation.

Dom34 releases ribosome stalled on the exogenous mRNA

Dom34 was reported to recognize and release stalled ribosomes on aberrant mRNAs to trigger mRNA decay. Here, we have shown that Dom34 mediates degradation of exogenous mRNA in a manner dependent on translation. Therefore, a parsimonious explanation for this observation is that the ribosome stalls on exogenous mRNA during translation and Dom34 recognizes this stalled ribosome to trigger the exogenous mRNA decay. To test this idea, we examined the polysomal distribution of the exogenous mRNA by polysome profile analysis. HeLa cells were depleted of Dom34 for 48 h and then transfected with 5×Flag-EGFP mRNA. The cell extract was fractionated by sucrose-density gradient centrifugation to separate the polysomes. RNAs extracted from polysomal fractions were subjected to northern blot analysis or ethidium bromide staining (Figure 5C). Knockdown of Dom34 resulted in a 2.4-fold increase in the level of 5×Flag-EGFP mRNA in the polysomal fractions without affecting the level of β-actin mRNA (Figure 5C, D). The result is consistent with our model suggesting that ribosomes stall on the exogenous mRNA, and Dom34 recognizes and releases the stalled ribosomes, which leads to the simultaneous decay of the exogenous mRNA.

Active RNase L dimer preferentially forms a complex with Dom34

Analogous to the mRNA quality control system, Dom34 recognizes a stalled ribosome on the exogenous mRNA and mediates degradation of exogenous mRNA in a manner dependent on translation. Considering this, together with the fact that Dom34 directly binds to RNase L, it is reasonable to think that Dom34 recruits RNase L to the stalled ribosome. Previous studies demonstrated that OAS-produced signaling 2–5A molecules convert RNase L from an inactive monomer to an active dimer (45,46). Thus, we examined if the interaction between RNase L and Dom34 depends on dimerization of RNase L. To test this idea, we constructed the RNase L Y312A mutant, which has mutation in Y312 involved in direct contact with 2–5A and fails to dimerize or to cleave RNA (47), and the interaction between RNase L and Dom34 was analyzed using an immunoprecipitation assay. HeLa cells were co-transfected with a plasmid expressing 5×Myc-Dom34 and a plasmid expressing either 5×Flag-RNase L or 5×Flag-RNase L Y312A, and the cell extracts were subjected to immunoprecipitation with an anti-Flag antibody. As compared with the wild-type 5×Flag-RNase L, the binding with 5×Myc-Dom34 was reduced 2.5-fold in the dimerization mutant 5×Flag-RNase L Y312A (Figure 6A, compare lanes 5 and 6; and 6B). These results suggest that dimerization/activation of RNase L promotes the interaction between RNase L and Dom34, and targeting RNase L to the translating exogenous mRNA. To confirm this, we next examined if an active RNase L dimer localizes to the polysome. HeLa cells were transfected with a plasmid expressing either 5×Flag-RNase L wt or 5×Flag-RNase L Y312A. At 24 h after transfection, the cells were further transfected with 5×Flag-EGFP mRNA. The cell lysates were fractionated by sucrose density gradients (Supplementary Figure S6A). Immunoblot analysis showed tendency of RNase L wt to be shifted from non-polysome to polysome fractions by the presence of exogenous mRNA, whereas RNase L Y312A localized to the non-polysomal fractions irrespective of whether the exogenous mRNA was present or not (Supplementary Figure S6A). However, quantitation of the results did not reach statistical significance provably because of the partial activation of RNase L by the exogenous mRNA (Supplementary Figure S6B and S6C). Therefore, we further assessed the effect of potent RNase L activator 2–5A on the polysomal localization of RNase L. HeLa/5×Flag-RNase L cells were transfected with 2–5A and the cell lysates were fractionated by sucrose density gradients (Figure 6C). Immunoblot analysis revealed that localization of endogenous RNase L was significantly shifted from non-polysome to polysome fractions by 2–5A (Figure 6D). These results suggest that dimerization/activation of RNase L promotes targeting of RNase L to the translating ribosome.

DISCUSSION

Here, we demonstrate that a well-known mRNA quality control factor, Dom34, as well as innate immune system OAS3-RNase L acts together to eliminate exogenous mRNA based on the following observations (see also Figure 6E); (i) OAS3 specifically binds to recognize exogenous mRNA (Figure 4C), (ii) exogenous mRNA activates 2′-5′ oligoadenylate synthetase activity of OAS3 to produce 2–5A (Figure 4D), (iii) 2–5A molecules convert RNase L from an inactive monomer to an active dimer (45,46), (iv) RNase L, but not its mutant that is unable to form an active dimer, prominently binds to form a complex with Dom34 (Figure 6A, B), (v) Dom34 and RNase L act together to degrade exogenous mRNA (Figure 3), (vi) translation is required for the decay of exogenous mRNA (Figure 5A, B) and (vii) Dom34 releases the stalled ribosome on exogenous mRNA (Figure 5C, D). From these results, we proposed the following model (Figure 6E); when exogenous mRNA enters into the cell cytosol, OAS3, activated by the mRNA, releases 2–5A, which in turn activates RNase L. The activated RNase L dimer binds Dom34 to form a surveillance complex. Meanwhile, the exogenous mRNA that entered the

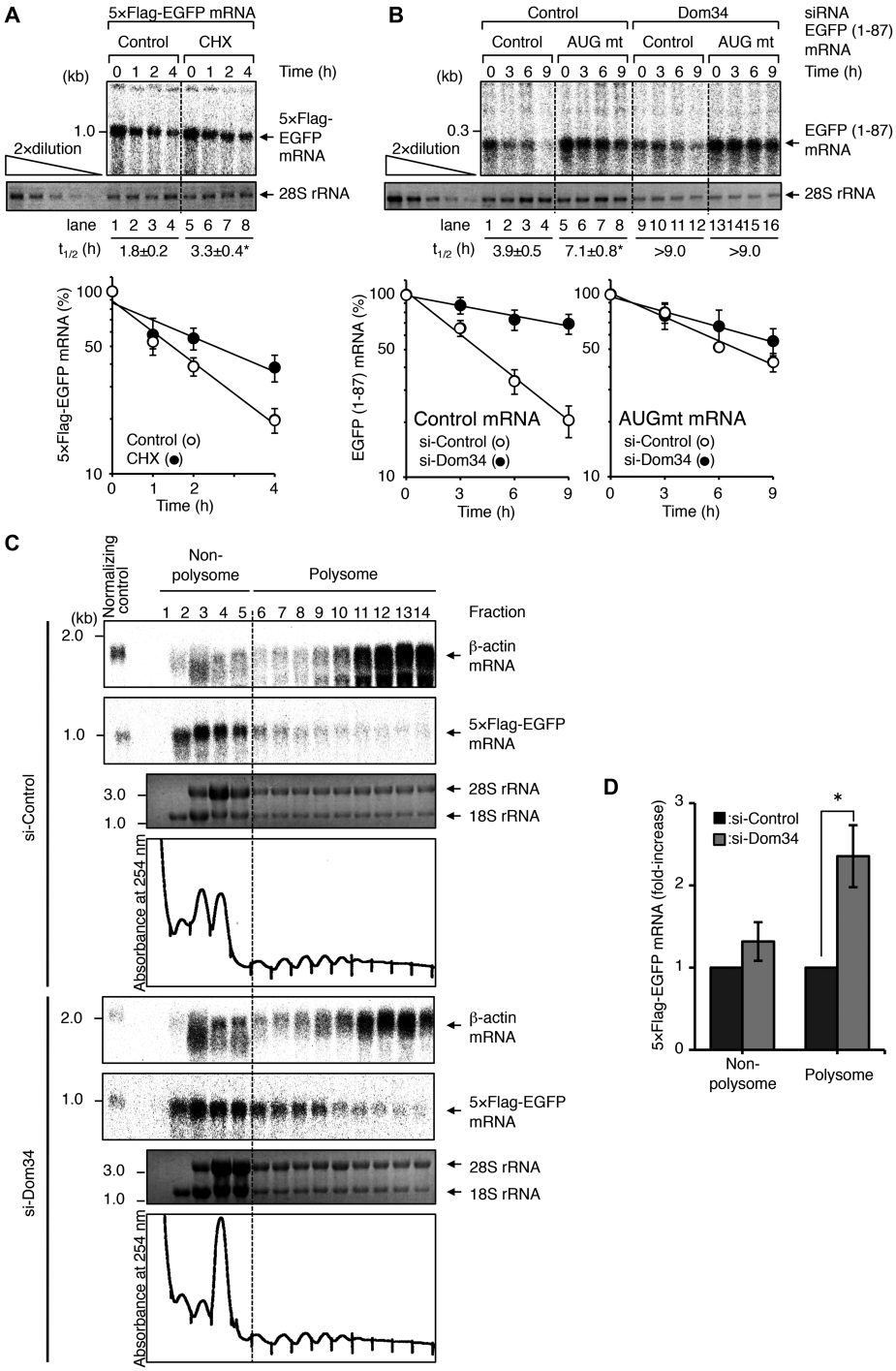

Figure 5. Degradation of exogenous mRNA requires translation. (**A**) HeLa cells were transfected with 5×Flag-EGFP mRNA for 3 h. The cells were treated with (lanes 5–8) or without (lanes 1–4) 200 μg/ml cycloheximide (CHX) and cultured in growth medium over time. 5×Flag-EGFP mRNA and 28S rRNA were analyzed by northern blotting and ethidium bromide staining, respectively. 5×Flag-EGFP mRNA decay was analyzed as in Figure 3E (mean ± SEM, $n = 3$), and the half-lives of 5×Flag-EGFP mRNA were calculated (average $t_{1/2}$ ± SEM, $n = 3$). (**B**) HeLa cells were transfected with siRNA against either luciferase (control) or Dom34. At 48 h after siRNA transfection, the cells were further transfected with control EGFP (1–87) mRNA (lanes 1–4 and 9–12) or EGFP (1–87)-(AUG mt) mRNA (lanes 5–8 and 13–16) for 3 h, and the cells were cultured in growth medium over time. EGFP (1–87) mRNA and 28S rRNA were analyzed by northern blotting and ethidium bromide staining, respectively. The leftmost five lanes, which analyzed 2-fold dilutions of total RNA, show that the conditions used for ethidium bromide staining are semi-quantitative. EGFP (1–87) mRNA decay was analyzed as in Figure 3E (mean ± SEM, $n = 4$), and the half-lives of EGFP (1–87) mRNA were calculated (average $t_{1/2}$ ± SEM, $n = 4$). (**C**) HeLa cells were transfected with siRNA against either control luciferase (upper panels) or Dom34 (lower panels). At 48 h after siRNA transfection, the cells were further transfected with 5×Flag-EGFP mRNA. At 3 h after mRNA transfection, the cells were lysed in buffer F. The cell lysates were fractionated by sucrose gradients. 5×Flag-EGFP mRNA and β-actin mRNA were analyzed by northern blotting, and 18S rRNA and 28S rRNA were analyzed by ethidium bromide staining. (**D**) Quantification of 5×Flag-EGFP mRNA in non-polysome (fractions 1–5) and polysome (fractions 6–14) in (C). The mRNA level in luciferase siRNA-treated cells was set to 1 and fold-increases are indicated (mean ± SEM, $n = 3$).

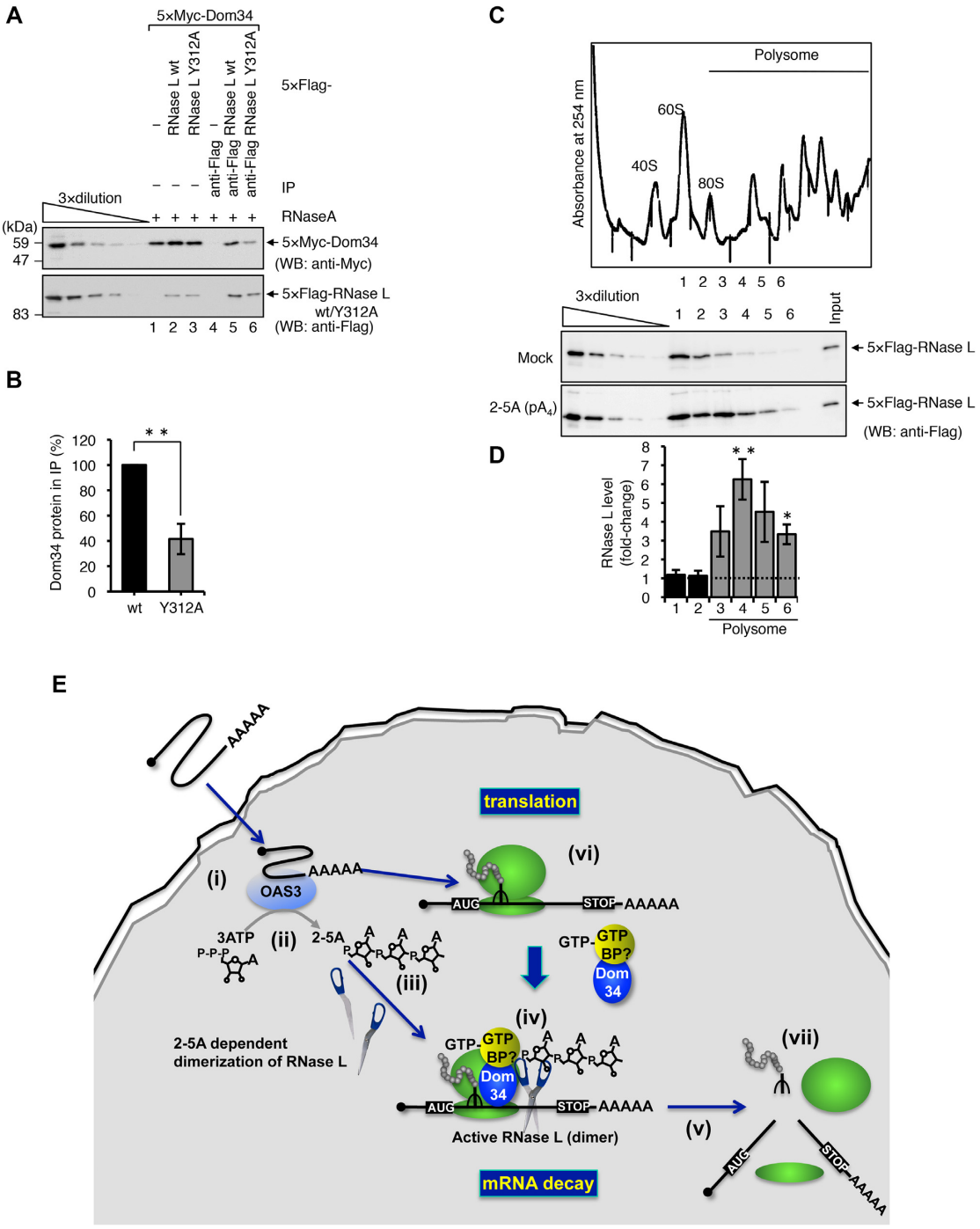

Figure 6. An active RNase L dimer preferentially localizes to the polysome to form a complex with Dom34. (**A**) HeLa cells were transfected with a combination of pCMV-5×Myc-Dom34 (lanes 1–6) and either pCMV-5×Flag (lanes 1 and 4), pCMV-5×Flag-RNase L (lanes 2 and 5) or pCMV-5×Flag-RNase L Y312A (lanes 3 and 6). The cells were lysed in buffer B. The immunoprecipitates (lanes 4–6) and inputs (lanes 1–3, 10% of the amount immunoprecipitated) were analyzed by western blotting with the indicated antibodies. The leftmost five lanes, which analyzed 3-fold dilutions of total protein, show that the conditions used for western blotting are semi-quantitative. (**B**) The amount of immunoprecipitated 5×Myc-Dom34 protein in (A) was measured and normalized to the input 5×Myc-Dom34 protein, and either immunoprecipitated 5×Flag-RNase L wt or RNase L Y312A. Dom34 protein level in pCMV-5×Flag-RNase L wt-transfected cells (lane 5) was defined as 100% and Dom34 protein level in pCMV-5×Flag-RNase L Y312A-transfected cells (lane 6) was represented. (**C**) HeLa/5×Flag-RNase L cells were transfected with 2–5A using Neon™ Transfection System. At 6 h after 2–5A electroporation, the cells were harvested and lysed in buffer G. The cell lysate was fractionated by sucrose gradients. 5×Flag-RNase L in the polysomal fractions and the input (0.5% of the amount loaded onto sucrose gradients) was analyzed by western blotting with an anti-Flag antibody. (**D**) The amount of endogenous 5×Flag-tagged RNase L protein in (**C**) was measured and normalized to the input. RNase L protein levels in mock cells were set to 1 and fold-changes were indicated (mean ± SEM, $n = 3$). (**E**) Model for the Dom34-mediated decay of exogenous mRNA (see Discussion).

cytosol is translated by the ribosome, which is recognized and targeted for degradation by the surveillance complex Dom34-RNase L (dimer).

Currently, viral and bacterial mRNAs are known to be degraded by the OAS-RNase L system. However, the mechanism by which the exogenous mRNAs are targeted for degradation by OAS-RNase L has yet to be determined. Here, we show for the first time that an mRNA surveillance factor, Dom34, plays a key role in driving the specificity of RNase L targeting. Previous studies demonstrated that Dom34 recognizes and releases a stalled ribosome on aberrant mRNAs to trigger mRNA decay (15,48). When aberrant mRNA lacking in-frame termination codons is translated by the ribosome, ribosome stalls at the 3′ poly(A) tail of the mRNA. Dom34 recognizes the stalled ribosomes and recruits exosomes to exonucleolytically degrade the mRNA by a mechanism of nonstop decay (NSD) (15,16). On the other hand, aberrant mRNA with a propensity to cause ribosomal stalling in the open reading frame (ORF) of the mRNA is degraded by a mechanism of no-go decay (NGD) (17). In this case, Dom34 recognizes the ribosome stalled in the ORF and triggers endonucleolytic cleavage of the mRNA by an unknown endonuclease. The exogenous mRNAs used in this study contain an ORF and cannot be a substrate for NSD. Accordingly, it is reasonable to assume that as in the case with NGD, the ribosome must be stalled within the ORF of the mRNA, and therefore, Dom34 recognizes the stalled ribosome to trigger endonucleolytic cleavage by RNase L. As the exogenous RNAs used in this study do not contain any apparent structural features to cause ribosomal stalling in their ORFs, we consider that the 'exogenous' nature of mRNA causes ribosomal stalling in its ORF for the following reasons. Endogenous mRNA experiences transcription and splicing events in the nucleus and binds splicing factors and hnRNPs to form an RNP complex. The 'nuclear history' determines the translational efficiency of cytoplasmic mRNA (49). In contrast, exogenous mRNA directly introduced into the cytosol can neither experience nuclear history nor form a translationally active RNP complex. Consistent with this RNP complex formation of endogenous mRNA, recent findings demonstrate that *in vivo* transcribed endogenous mRNAs have vastly fewer structured regions than mRNAs *in vitro* (50). Thus, exogenous mRNA is translationally inefficient and tends to form a secondary structure, which may cause ribosomal stalling. The secondary structure formed in the exogenous mRNA is also an attractive target of OAS. Therefore, it is interesting to speculate that the secondary structure formed in the exogenous mRNA leads to the localized activation of OAS as well as ribosomal stalling, and 2–5A released from the OAS binds to activate RNase L, which is recruited by Dom34 on the stalled ribosome. Further studies will be required for elucidating if activation of OAS3 and ribosomal stalling is induced by the same structured regions formed on exogenous mRNA

It is well-established that mRNA decay is tightly coupled to translation. In NMD, the translation termination factor complex eRF1–eRF3 recognizes the terminating ribosome at the premature termination codon to triggers rapid degradation. In contrast, a *bona fide* termination codon is efficiently recognized by the eRF1–eRF3 in complex with poly(A) binding protein and eRF1–eRF3 mediates recruitment of the deadenylases to PABP to trigger deadenylation of the mRNA. In NSD, the ribosome that entered into the 3′ poly(A) tail of the mRNA and stalled at the 3′ end is recognized by Dom34 in complex with Hbs1, which leads to the recruitment of exosomes to degrade the mRNA. In this study, we have shown that exogenous mRNA is also recognized and targeted for degradation by Dom34 in a manner dependent on translation. Therefore, irrespective of whether endogenous or exogenous, mRNA is commonly targeted for degradation by the translation termination factor family members. Although undetermined, it is reasonable to assume that a member of the eRF3 family GTP-binding proteins is also involved in the exogenous mRNA decay. A previous study showed that RNase L interacts with eRF3 (51). Moreover, recent findings demonstrate that Dom34 interacts with a recycling factor, ABCE1, which dissociates ribosome into subunits, after recognition of the stalled ribosome (47,52,53). Interestingly, ABCE1 is also referred to as an RNase L inhibitor (54). Therefore, it is interesting to speculate that ABCE1 might also affect exogenous mRNA decay. These possibilities are now under investigation in our laboratory.

SUPPLEMENTARY DATA

Supplementary Data are available at NAR Online.

ACKNOWLEDGEMENTS

We thank Dr Satoshi Koike and Dr Narushi Iizuka for plasmids.

Author contributions: T.No., K.N., S.K., N.H., S.H. designed the experiments; T.No., K.N., S.K., T.Na., Y.O. performed the experiments; H.I. provided EMCV constructs and technical support; Y.K., Y.K. provided 2–5A and presented comments; T.No., S.H. wrote the paper; S.H. conceived and directed the study.

FUNDING

JSPS Grant-in-Aid for Scientific Research (B) [JP17H03635 to S.H.]; JSPS Challenging Research (Exploratory) [JP17K19357 to S.H.]; Program on the Innovative Development and the Application of New Drugs for Hepatitis B from Japan Agency for Medical Research and development, AMED [JP17fk0310111 to S.H]; TAKEDA Science foundation [JOSEI32912 to S.H.]; Grant-in-Aid Research in Nagoya City University [No. 6 to S.H.]. Funding for open access charge: Program on the Innovative Development and the Application of New Drugs for Hepatitis B from Japan Agency for Medical Research and development, AMED [JP17fk0310111].

Conflict of interest statement. None declared.

REFERENCES

1. Mata,J., Marguerat,S. and Bähler,J. (2005) Post-transcriptional control of gene expression: a genome-wide perspective. *Trends Biochem. Sci.*, **30**, 506–514.
2. Hsu,C.L. and Stevens,A. (1993) Yeast cells lacking 5′–>3' exoribonuclease 1 contain mRNA species that are poly(A) deficient and partially lack the 5′ cap structure. *Mol. Cell. Biol.*, **13**, 4826–4835.

3. Muhlrad,D., Decker,C.J. and Parker,R. (1994) Deadenylation of the unstable mRNA encoded by the yeast MFA2 gene leads to decapping followed by 5′–>3' digestion of the transcript. *Genes Dev.*, **8**, 855–866.
4. Shyu,A.B., Belasco,J.G. and Greenberg,M.E. (1991) Two distinct destabilizing elements in the c-fos message trigger deadenylation as a first step in rapid mRNA decay. *Genes Dev.*, **5**, 221–231.
5. Decker,C.J. and Parker,R. (1993) A turnover pathway for both stable and unstable mRNAs in yeast: evidence for a requirement for deadenylation. *Genes Dev.*, **7**, 1632–1643.
6. Funakoshi,Y., Doi,Y., Hosoda,N., Uchida,N., Osawa,M., Shimada,I., Tsujimoto,M., Suzuki,T., Katada,T. and Hoshino,S. (2007) Mechanism of mRNA deadenylation: evidence for a molecular interplay between translation termination factor eRF3 and mRNA deadenylases. *Genes Dev.*, **21**, 3135–3148.
7. Hoshino,S. (2012) Mechanism of the initiation of mRNA decay: role of eRF3 family G proteins. *Wiley Interdiscip. Rev. RNA*, **3**, 743–757.
8. Pelechano,V., Wei,W. and Steinmetz,L.M. (2015) Widespread co-translational rna decay reveals ribosome dynamics. *Cell*, **161**, 1400–1412.
9. Hu,W., Sweet,T.J., Chamnongpol,S., Baker,K.E. and Coller,J. (2009) Co-translational mRNA decay in Saccharomyces cerevisiae. *Nature*, **461**, 225–229.
10. Karousis,E.D., Nasif,S. and Mühlemann,O. (2016) Nonsense-mediated mRNA decay: novel mechanistic insights and biological impact. *Wiley Interdiscip. Rev. RNA*, **7**, 661–682.
11. Popp,M.W. and Maquat,L.E. (2013) Organizing principles of mammalian nonsense-mediated mRNA decay. *Annu. Rev. Genet.*, **47**, 139–165.
12. Kashima,I., Yamashita,A., Izumi,N., Kataoka,N., Morishita,R., Hoshino,S., Ohno,M., Dreyfuss,G. and Ohno,S. (2006) Binding of a novel SMG-1-Upf1-eRF1–eRF3 complex (SURF) to the exon junction complex triggers Upf1 phosphorylation and nonsense-mediated mRNA decay. *Genes Dev*, **20**, 355–367.
13. Frischmeyer,P.A., van Hoof,A., O'Donnell,K., Guerrerio,A.L., Parker,R. and Dietz,H.C. (2002) An mRNA surveillance mechanism that eliminates transcripts lacking termination codons. *Science*, **295**, 2258–2261.
14. van Hoof,A., Frischmeyer,P.A., Dietz,H.C. and Parker,R. (2002) Exosome-mediated recognition and degradation of mRNAs lacking a termination codon. *Science*, **295**, 2262–2264.
15. Tsuboi,T., Kuroha,K., Kudo,K., Makino,S., Inoue,E., Kashima,I. and Inada,T. (2012) Dom34:hbs1 plays a general role in quality-control systems by dissociation of a stalled ribosome at the 3' end of aberrant mRNA. *Mol. Cell*, **46**, 518–529.
16. Saito,S., Hosoda,N. and Hoshino,S. (2013) The Hbs1-Dom34 protein complex functions in non-stop mRNA decay in mammalian cells. *J. Biol. Chem.*, **288**, 17832–17843.
17. Doma,M.K. and Parker,R. (2006) Endonucleolytic cleavage of eukaryotic mRNAs with stalls in translation elongation. *Nature*, **440**, 561–564.
18. Silverman,R.H. (2007) Viral encounters with 2',5′-oligoadenylate synthetase and RNase L during the interferon antiviral response. *J. Virol.*, **81**, 12720–12729.
19. Ireland,D.D., Stohlman,S.A., Hinton,D.R., Kapil,P., Silverman,R.H., Atkinson,R.A. and Bergmann,C.C. (2009) RNase L mediated protection from virus induced demyelination. *PLoS Pathog*, **5**, e1000602.
20. Jha,B.K., Polyakova,I., Kessler,P., Dong,B., Dickerman,B., Sen,G.C. and Silverman,R.H. (2011) Inhibition of RNase L and RNA-dependent protein kinase (PKR) by sunitinib impairs antiviral innate immunity. *J. Biol. Chem.*, **286**, 26319–26326.
21. Hovanessian,A.G., Brown,R.E. and Kerr,I.M. (1977) Synthesis of low molecular weight inhibitor of protein synthesis with enzyme from interferon-treated cells. *Nature*, **268**, 537–540.
22. Clemens,M.J. and Williams,B.R. (1978) Inhibition of cell-free protein synthesis by pppA2'p5′A2'p5′A: a novel oligonucleotide synthesized by interferon-treated L cell extracts. *Cell*, **13**, 565–572.
23. Kerr,I.M. and Brown,R.E. (1978) pppA2'p5′A2'p5′A: an inhibitor of protein synthesis synthesized with an enzyme fraction from interferon-treated cells. *Proc. Natl. Acad. Sci. U.S.A.*, **75**, 256–260.
24. Ratner,L., Wiegand,R.C., Farrell,P.J., Sen,G.C., Cabrer,B. and Lengyel,P. (1978) Interferon, double-stranded RNA and RNA degradation. Fractionation of the endonucleaseINT system into two macromolecular components; role of a small molecule in nuclease activation. *Biochem. Biophys. Res. Commun.*, **81**, 947–954.
25. Slattery,E., Ghosh,N., Samanta,H. and Lengyel,P. (1979) Interferon, double-stranded RNA, and RNA degradation: activation of an endonuclease by (2'-5′)An. *Proc. Natl. Acad. Sci. U.S.A.*, **76**, 4778–4782.
26. Baglioni,C., De Benedetti,A. and Williams,G.J. (1984) Cleavage of nascent reovirus mRNA by localized activation of the 2'-5′-oligoadenylate-dependent endoribonuclease. *J. Virol.*, **52**, 865–871.
27. Nilsen,T.W. and Baglioni,C. (1979) Mechanism for discrimination between viral and host mRNA in interferon-treated cells. *Proc. Natl. Acad. Sci. U.S.A.*, **76**, 2600–2604.
28. Li,X.L., Blackford,J.A. and Hassel,B.A. (1998) RNase L mediates the antiviral effect of interferon through a selective reduction in viral RNA during encephalomyocarditis virus infection. *J. Virol.*, **72**, 2752–2759.
29. Kobayashi,T., Mikami,S., Yokoyama,S. and Imataka,H. (2007) An improved cell-free system for picornavirus synthesis. *J. Virol. Methods*, **142**, 182–188.
30. Hosoda,N., Funakoshi,Y., Hirasawa,M., Yamagishi,R., Asano,Y., Miyagawa,R., Ogami,K., Tsujimoto,M. and Hoshino,S. (2011) Anti-proliferative protein Tob negatively regulates CPEB3 target by recruiting Caf1 deadenylase. *EMBO J.*, **30**, 1311–1323.
31. Ruan,L., Osawa,M., Hosoda,N., Imai,S., Machiyama,A., Katada,T., Hoshino,S. and Shimada,I. (2010) Quantitative characterization of Tob interactions provides the thermodynamic basis for translation termination-coupled deadenylase regulation. *J. Biol. Chem.*, **285**, 27624–27631.
32. Hoshino,S., Imai,M., Mizutani,M., Kikuchi,Y., Hanaoka,F., Ui,M. and Katada,T. (1998) Molecular cloning of a novel member of the eukaryotic polypeptide chain-releasing factors (eRF). Its identification as eRF3 interacting with eRF1. *J. Biol. Chem.*, **273**, 22254–22259.
33. Hoshino,S., Imai,M., Kobayashi,T., Uchida,N. and Katada,T. (1999) The eukaryotic polypeptide chain releasing factor (eRF3/GSPT) carrying the translation termination signal to the 3'-Poly(A) tail of mRNA. Direct association of erf3/GSPT with polyadenylate-binding protein. *J. Biol. Chem.*, **274**, 16677–16680.
34. Meng,H., Deo,S., Xiong,S., Dzananovic,E., Donald,L.J., van Dijk,C.W. and McKenna,S.A. (2012) Regulation of the interferon-inducible 2'-5′-oligoadenylate synthetases by adenovirus VA(I) RNA. *J. Mol. Biol.*, **422**, 635–649.
35. Chakrabarti,A., Jha,B.K. and Silverman,R.H. (2011) New insights into the role of RNase L in innate immunity. *J. Interferon Cytokine Res.*, **31**, 49–57.
36. Balistreri,G., Horvath,P., Schweingruber,C., Zünd,D., McInerney,G., Merits,A., Mühlemann,O., Azzalin,C. and Helenius,A. (2014) The host nonsense-mediated mRNA decay pathway restricts Mammalian RNA virus replication. *Cell Host Microbe*, **16**, 403–411.
37. Hahn,H. and Palmenberg,A.C. (1995) Encephalomyocarditis viruses with short poly(C) tracts are more virulent than their mengovirus counterparts. *J. Virol.*, **69**, 2697–2699.
38. Svitkin,Y.V. and Sonenberg,N. (2003) Cell-free synthesis of encephalomyocarditis virus. *J. Virol.*, **77**, 6551–6555.
39. Shoemaker,C.J., Eyler,D.E. and Green,R. (2010) Dom34:Hbs1 promotes subunit dissociation and peptidyl-tRNA drop-off to initiate no-go decay. *Science*, **330**, 369–372.
40. Harigaya,Y. and Parker,R. (2010) No-go decay: a quality control mechanism for RNA in translation. *Wiley Interdiscip. Rev. RNA*, **1**, 132–141.
41. Han,J.Q., Townsend,H.L., Jha,B.K., Paranjape,J.M., Silverman,R.H. and Barton,D.J. (2007) A phylogenetically conserved RNA structure in the poliovirus open reading frame inhibits the antiviral endoribonuclease RNase L. *J. Virol.*, **81**, 5561–5572.
42. Thakur,C.S., Xu,Z., Wang,Z., Novince,Z. and Silverman,R.H. (2005) A convenient and sensitive fluorescence resonance energy transfer assay for RNase L and 2',5′ oligoadenylates. *Methods Mol. Med.*, **116**, 103–113.
43. Hovanessian,A.G. (2007) On the discovery of interferon-inducible, double-stranded RNA activated enzymes: the 2'-5′oligoadenylate synthetases and the protein kinase PKR. *Cytokine Growth Factor Rev.*, **18**, 351–361.

44. Donovan,J., Whitney,G., Rath,S. and Korennykh,A. (2015) Structural mechanism of sensing long dsRNA via a noncatalytic domain in human oligoadenylate synthetase 3. *Proc. Natl. Acad. Sci. U.S.A.*, **112**, 3949–3954.
45. Cole,J.L., Carroll,S.S. and Kuo,L.C. (1996) Stoichiometry of 2',5′-oligoadenylate-induced dimerization of ribonuclease L. A sedimentation equilibrium study. *J. Biol. Chem.*, **271**, 3979–3981.
46. Dong,B. and Silverman,R.H. (1995) 2–5A-dependent RNase molecules dimerize during activation by 2–5A. *J. Biol. Chem.*, **270**, 4133–4137.
47. Han,Y., Donovan,J., Rath,S., Whitney,G., Chitrakar,A. and Korennykh,A. (2014) Structure of human RNase L reveals the basis for regulated RNA decay in the IFN response. *Science*, **343**, 1244–1248.
48. Pisareva,V.P., Skabkin,M.A., Hellen,C.U., Pestova,T.V. and Pisarev,A.V. (2011) Dissociation by Pelota, Hbs1 and ABCE1 of mammalian vacant 80S ribosomes and stalled elongation complexes. *EMBO J.*, **30**, 1804–1817.
49. Matsumoto,K., Wassarman,K.M. and Wolffe,A.P. (1998) Nuclear history of a pre-mRNA determines the translational activity of cytoplasmic mRNA. *EMBO J.*, **17**, 2107–2121.
50. Rouskin,S., Zubradt,M., Washietl,S., Kellis,M. and Weissman,J.S. (2014) Genome-wide probing of RNA structure reveals active unfolding of mRNA structures in vivo. *Nature*, **505**, 701–705.
51. Le Roy,F., Salehzada,T., Bisbal,C., Dougherty,J.P. and Peltz,S.W. (2005) A newly discovered function for RNase L in regulating translation termination. *Nat Struct Mol. Biol.*, **12**, 505–512.
52. Becker,T., Franckenberg,S., Wickles,S., Shoemaker,C.J., Anger,A.M., Armache,J.P., Sieber,H., Ungewickell,C., Berninghausen,O., Daberkow,I. *et al.* (2012) Structural basis of highly conserved ribosome recycling in eukaryotes and archaea. *Nature*, **482**, 501–506.
53. Shoemaker,C.J. and Green,R. (2011) Kinetic analysis reveals the ordered coupling of translation termination and ribosome recycling in yeast. *Proc. Natl. Acad. Sci. U.S.A.*, **108**, E1392–E1398.
54. Bisbal,C., Martinand,C., Silhol,M., Lebleu,B. and Salehzada,T. (1995) Cloning and characterization of a RNAse L inhibitor. A new component of the interferon-regulated 2–5A pathway. *J. Biol. Chem.*, **270**, 13308–13317.